

c. 1  
17153

THE REACTION OF SINGLET OXYGEN  
WITH OLEFINS

BY

ROBERT D. ASHFORD

B.Sc. (Hons.), University of London, England, 1967  
M.Sc., University of British Columbia, 1970

A THESIS SUBMITTED IN PARTIAL FULFILMENT OF  
THE REQUIREMENTS FOR THE DEGREE OF  
DOCTOR OF PHILOSOPHY  
in the Department  
of  
Chemistry

We accept this thesis as conforming to the  
required standard

THE UNIVERSITY OF BRITISH COLUMBIA

September, 1973

In presenting this thesis in partial fulfilment of the requirements for an advanced degree at the University of British Columbia, I agree that the Library shall make it freely available for reference and study. I further agree that permission for extensive copying of this thesis for scholarly purposes may be granted by the Head of my Department or by his representatives. It is understood that copying or publication of this thesis for financial gain shall not be allowed without my written permission.

Department of Chemistry.

The University of British Columbia  
Vancouver 8, Canada

Date 17/Sept/73.

# ABSTRACT

The reaction of singlet oxygen with a number of substituted mono- and di-olefins was studied here in the gas phase. The reaction took place in a conventional discharge flow system and was followed by a mass spectrometer which measured the decay of the olefin concentration along the tube. The singlet oxygen was monitored photometrically using a calibrated photomultiplier tube.

By determination of the rate constant at a series of temperatures up to 200°C, it was possible to obtain a value for the activation energy and entropy change for each compound, and so gain an idea of the different chemical influences that govern the rate of reaction. It was found that increased methyl substitution caused a lowering of the activation energy, and that the mono-methyl and unsubstituted derivatives of cyclohexene appeared to have an anomalously high activation energy in comparison with the cyclopentene or butene-2 analogues. These influences were interpreted in the light of the 'ene' mechanism for the mono-olefins. In the case of the dienes, the evidence points to a normal Diels-Alder type addition reaction. A detailed description of the transition states for these two reactions is given.

The entropy change for the reaction was found to remain approximately constant with the different olefins and was correlated with the calculated values for the different intermediates and transition states that have been proposed for these reactions. It was pointed out that the disparity with the data obtained in solution is such that a simple

transfer of these conclusions to other systems must be treated with a considerable amount of caution.

TABLE OF CONTENTS

	<u>Page</u>
ABSTRACT .....	ii
TABLE OF CONTENTS .....	iv
LIST OF TABLES .....	vi
LIST OF ILLUSTRATIONS .....	vii
ACKNOWLEDGEMENTS .....	viii
 INTRODUCTION .....	 1
The Electronic Structure of Molecular Oxygen .....	2
Spectroscopic Studies .....	3
The Production of Singlet Oxygen .....	8
Quenching of Singlet Oxygen .....	10
Reaction of Singlet Oxygen with Olefins .....	11
Gas Phase Reaction Studies .....	17
 EXPERIMENTAL .....	 23
The Discharge-Flow System .....	23
The Microwave Discharge .....	26
The Mass Spectrometer .....	27
Determination of the $O_2(^1\Delta_g)$ Concentration .....	32
Chemicals .....	35
 RESULTS .....	 37
The Temperature Dependence of the $O_2(^1\Delta_g)$ -Olefin Reaction .....	40
The Pressure Dependence of the $O_2(^1\Delta_g)$ -2,3-dimethyl butene-2 Reaction .....	74

	<u>Page</u>
DISCUSSION .....	77
Comparison with $O_2(^1\Delta_g)$ Decay Studies .....	77
Comparison with Other Temperature Dependence Studies ..	79
The Entropy of the Transition State .....	83
The Transition State of the $O_2(^1\Delta_g)$ -Olefin Reaction ...	87
The Transition State of the $O_2(^1\Delta_g)$ -Diene Reaction ....	92
CONCLUSIONS .....	95
REFERENCES .....	96

LIST OF TABLES

<u>Table</u>		<u>Page</u>
1	Observed transitions between low-lying excited state of molecular oxygen .....	5
2	Observed double molecule transitions in oxygen.....	7
3	The quenching efficiencies of $O_2(^1\Delta_g)$ by different compounds .....	12
4	Rate constants for reaction of singlet oxygen with olefins at room temperature .....	21
5-17	The data used to calculate the rate constants at each temperature .....	42-54
18	The preexponential factors and activation energies for the $O_2(^1\Delta_g)$ -olefin reaction .....	69
19	Rate constants for the $O_2(^1\Delta_g)$ -2,3-dimethyl butene-2 reaction at different pressures .....	75
20	A comparison of the rate constants for reaction ( $K_r$ ) and quenching ( $K_q$ ) in the $O_2(^1\Delta_g)$ -olefin system at 25°C.....	78
21	A comparison of the solution and gas phase temperature dependence data .....	81
22	The enthalpy and entropy changes in the reaction of $O_2(^1\Delta_g)$ with 2,3-dimethyl butene-2 and cyclopentadiene .....	84
23	The estimated entropy changes for the proposed intermediates in the $O_2(^1\Delta_g)$ -2,3-dimethyl butene-2 reaction .....	86

LIST OF ILLUSTRATIONS

<u>Figure</u>		<u>Page</u>
1	The oxygen potential energy diagram as compiled by Gilmore .....	4
2	The spectrum of singlet oxygen between 8000 Å and 3500 Å as obtained by Gray and Ogryzlo .....	6
3	A diagram of the flowtube used in this work .....	24
4	Schematic diagram of electronic used to control the quadrupole mass spectrometer .....	29
5	A diagram of the mass spectrometer pumping arrangement .....	31
6	The circuit of the isothermal calorimeter .....	33
7	The relationship between the peak height observed in the mass spectrometer and the partial pressure within the flowtube for argon .....	39
8	Plots of $\log(H_o/H)$ vs. time .....	41
9-21	Arrhenius plots: $\log k_r$ vs. $1/T$ .....	55-67
22-25	Arrhenius plots: $\log k_r$ vs. $1/T$ on smaller scale.	70-73

#### ACKNOWLEDGEMENTS

The research described in this thesis was performed under the auspices of the Centre for Research in Atmospheric Photochemistry situated in Room 321 of the Chemistry Department at the University of British Columbia. The author would like to express his particular thanks to the director and research supervisor of that institution, Dr. E.A. Ogryzlo, and his immediate colleagues in the laboratory, Helen Lakusta and Jim Davidson.

Thanks are also due to the University of British Columbia for providing the mass spectrometer used in this work and to the Chemistry Department for providing research facilities.

Some helpful discussions with Dr. R.E. Pincock and Dr. J.R. Scheffer are gratefully acknowledged.

## INTRODUCTION

The intense interest that has been shown in the chemical and physical properties of singlet oxygen over the last decade has now produced a general awareness that this is an excited state that is not simply confined to the specialized realms of the emission spectroscopist, but one that is also found in many systems of interest to the modern chemist. The major portion of the credit for this discovery must go to those organic chemists interested in the mechanism for the olefin photooxidation process in which singlet oxygen is present as an intermediate. It was during the course of their early work in this area that the discussion arose concerning the nature of the mechanism for the final oxidation reaction that has been so prevalent in the singlet oxygen literature of recent years. This dispute has not yet been fully resolved.

The work to be presented in this thesis is a gas phase kinetic study of these reactions which, it is hoped, will aid in clearing up some of the misunderstanding that has surrounded this subject as well as provide a quantitative foundation for a physical interpretation of the mechanism.

### The Electronic Structure of Molecular Oxygen

Molecular oxygen in its un-ionized state consists of 16 electrons arranged according to the Pauli and Aufbau principles in the different molecular orbitals formed by the LCAO approximation:-

$$(\sigma 1s)^2 (\sigma^* 1s)^2 (\sigma 2s)^2 (\sigma^* 2s)^2 (\sigma 2p)^2 (\pi 2p)^4 (\pi^* 2p)^2 \quad (1)$$

The three lowest lying excited states of the molecule can be represented by the different conformations of the two electrons in the half-filled anti-bonding orbitals, and are each expressed by wave functions composed of separate spin and orbital terms (2-5):-

$${}^1\Sigma_g^+ = \frac{1}{\sqrt{2}} (\pi_{+1}^*(1) \pi_{-1}^*(2) + \pi_{-1}^*(2) \pi_{+1}^*(1)) (\alpha(1)\beta(2) - \alpha(2)\beta(1)) \quad (2)$$

$${}^1\Delta_g = \begin{cases} \pi_{+1}^*(1) \pi_{+1}^*(2) (\alpha(1)\beta(2) - \alpha(2)\beta(1)) \\ \pi_{-1}^*(1) \pi_{-1}^*(2) (\alpha(1)\beta(2) - \alpha(2)\beta(1)) \end{cases} \quad (3)$$

$${}^3\Sigma_g^- = \begin{cases} \frac{1}{\sqrt{2}} (\pi_{+1}^*(1) \pi_{-1}^*(2) - \pi_{+1}^*(2) \pi_{-1}^*(1)) \\ \begin{pmatrix} \alpha(1)\alpha(2) \\ \alpha(1)\beta(2) + \alpha(2)\beta(1) \\ \beta(1)\beta(2) \end{pmatrix} \end{cases} \quad (4)$$

where  $\alpha$  and  $\beta$  represent the electron spin and  $\pi_{+1}^*(1)$ , the wave function of electron (1) in the  $\pi^*$  state with  $\Lambda = +1$ . Here the  $X({}^3\Sigma_g^-)$  represents the ground state of the molecule, with the excited  $a({}^1\Delta_g)$  and  $b({}^1\Sigma_g^+)$  states lying respectively, 0.98 e.V. and 1.66 e.V. above this level

(Fig. 1). 'Singlet oxygen' refers to these two low lying excited states of molecular oxygen.

### Spectroscopic Studies

Both the ( $^1\Delta_g$ ) and ( $^1\Sigma_g^+$ ) states of oxygen were first observed by absorption of atmospheric oxygen in the red and infrared regions of the solar spectrum (5) and later, in the laboratory, using emission (6) and absorption techniques (7). All transitions are electric-dipole forbidden and therefore weak. The relevant features are given in Table 1.

Of particular interest in the chemistry of singlet oxygen are the double molecule energy pooling processes which give rise to emission in the visible region of the spectrum. The collision of two ( $^1\Delta_g$ ) molecules can produce, not only a collision-induced increase in radiation at  $1.27\ \mu$ , but also emission at  $6340\ \text{\AA}$ , corresponding to a photon with twice the usual ( $0,0$ )  $^1\Delta_g - ^3\Sigma_g^-$  energy. It is this transition that is responsible for both the characteristic red colour of gaseous singlet oxygen as well as the faint blue colour of liquid oxygen (8). A number of bands have been observed involving both ( $^1\Delta_g$ ) and ( $^1\Sigma_g^+$ ) as well as transitions from various vibrationally excited levels of these states (Fig. 2). They are listed in Table 2. together with their radiative lifetimes and wavelengths (9).

It was shown by Bader and Ogryzlo (10), and has since been verified in a number of other cases (11,12), that the intensity of the red  $6340\ \text{\AA}$  emission band is proportional to the square of the ( $^1\Delta_g$ ) concentration. It thus provides a conveniently accessible monitor of the  $O_2(^1\Delta_g)$  concentration and is used for this purpose in the present work.



Table 1. Observed transitions between the low-lying excited states of molecular oxygen.

Band	Transition	Origin	Type
Infrared atmospheric	$1\Delta_g - 3\Sigma_g^-$	7619 Å	mag. dipole
Red atmospheric	$1\Sigma_g^+ - 3\Sigma_g^-$	1.27 μ	mag. dipole
'Noxon'	$1\Sigma_g^+ - 1\Delta_g$	1.908 μ	elect. quadrupole

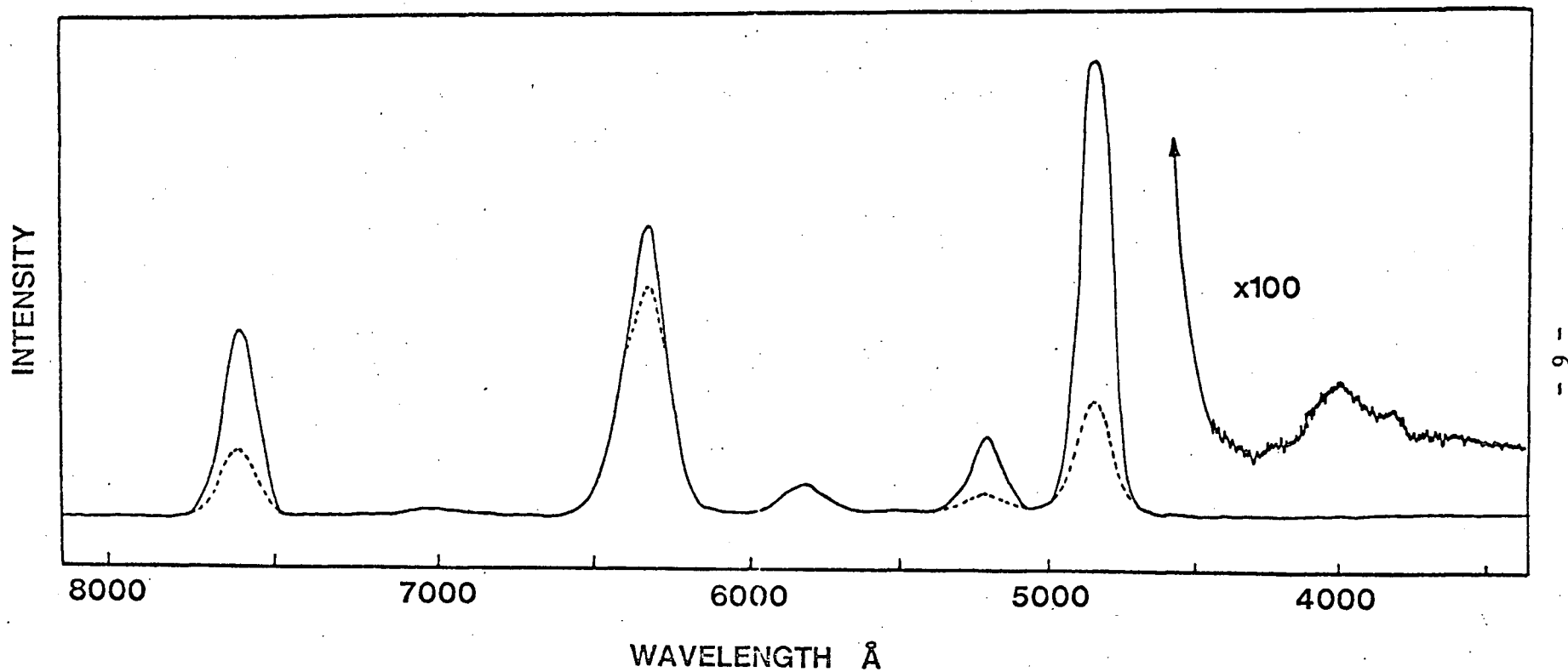


Figure 2. The emission spectrum of singlet oxygen between 8000 Å and 3500 Å as obtained by Gray and Ogryslø (9). Taken using an RCA 1P21 photomultiplier and is uncorrected for spectral response. The dotted line shows the relative spectra at 300°K and the solid line at 150°K. Both spectra were taken at 10 torr.

Table 2. Observed double molecule transitions in oxygen.

Excited state	Transition to ground ( $^3\Sigma_g^- + ^3\Sigma_g^-$ ) state		
	$\nu_{\text{excited}} - \nu_{\text{ground}}$	Wavelength ( $\text{\AA}$ )	Lifetime* (secs)
$^1\Delta_g + ^3\Sigma_g^-$	0	12700	4
	-1	15800	
$^1\Sigma_g^+ + ^3\Sigma_g^-$	0	7619	15
	-1	8345	
$^1\Delta_g + ^1\Delta_g$	0	6340	1.5
	-1	7030	
	+1	5800	
$^1\Delta_g + ^1\Sigma_g^+$	0	4800	1.7
	-1	5200	
$^1\Sigma_g^+ + ^1\Sigma_g^+$	0	4000	0.3
	-1	3800	

\* Calculated from integrated absorption coefficients (9).

## The Production of Singlet Oxygen

### (a) Triplet Energy Transfer

The possibility that a triplet sensitizer could undergo an energy transfer process to produce excited molecular oxygen was a suggestion originally put forward by Kautsky in 1939 (13) and since demonstrated to be correct in a wide variety of different systems (14,15). The process involves the excitation of the sensitizer into its first singlet excited state, followed by intersystem crossing to the triplet state and finally energy transfer to the oxygen. The excited oxygen is then rapidly removed by reaction with the acceptor molecule:



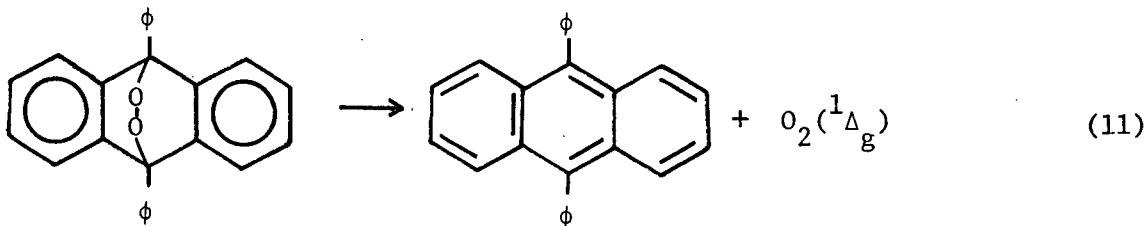
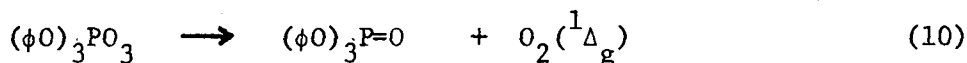
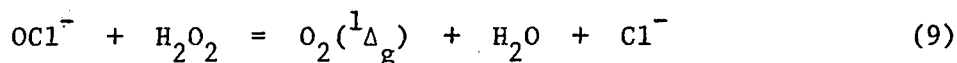
This theory is kinetically indistinguishable from one requiring the formation of a sensitizer-oxygen complex as the oxidising agent and it did not receive general acceptance until it was eventually shown in 1964 (16) that similar photooxidation products resulted from direct reaction with singlet oxygen produced by the  $OC\bar{I}^-/H_2O_2$  decomposition method. Since then, this technique has been extensively used for the routine production of singlet oxygen both in solution and in the gas phase.

Kearns has suggested (17) from a detailed examination of the Frank-Condon factors of the oxygen transitions, that sensitizers with a

triplet energy greater than ~40 Kcals, would produce a 10:1 ratio of  $O_2(^1\Sigma_g^+)$  to  $O_2(^1\Delta_g)$  in reaction (8), while triplet energies of less than this amount would produce the reverse case. It is fairly certain, however, that in most circumstances it is the  $O_2(^1\Delta_g)$  state that is involved in reaction with the acceptor (2). This is because, under the usual conditions of these reactions, the lifetime of the  $O_2(^1\Sigma_g^+)$  is so short that its contribution is insignificant compared with that of the  $O_2(^1\Delta_g)$ . This means that an  $O_2(^1\Sigma_g^+)$  reaction rate of at least 1000 times the  $O_2(^1\Delta_g)$  analogue would be required to make any appreciable effect on the product formation in reaction (8).

(b) Chemical Production

Three reactions are commonly employed as sources of  $O_2(^1\Delta_g)$ . These are as follows:-



In all three of these reactions the presence of singlet oxygen has been well established: In the first two cases this was achieved by direct spectroscopic observation of the  $O_2(^1\Delta_g)$  emission (18,19), while in the

third, which represents the decomposition of the stable product of a photooxidation reaction, the transfer of the peroxide group to another acceptor molecule was regarded as providing sufficient proof of this supposition (20).

### (c) Discharge Flow Systems

In the discharge flow technique for the production of singlet oxygen, a conventional microwave discharge is employed to excite the molecular oxygen into its singlet state. The excited oxygen is then removed from the discharge by pumping it along a tube where it is eventually allowed to react with the various added gases. Atomic oxygen, which is also produced by this technique, can be selectively removed from the stream by catalytic recombination on a surface of mercuric oxide produced by distilling a small quantity of mercury through the discharge region. Typically  $O_2(^1\Delta_g)$  and  $O_2(^1\Sigma_g^+)$  concentrations of  $\sim 10\%$  and  $\sim 0.1\%$  can be produced by such means, the concentration of other excited species being negligible.

The discharge flow technique is used for the study of the reactions described in the present work.

### Quenching of Singlet Oxygen

The rate constants for quenching of  $O_2(^1\Sigma_g^+)$  have been determined by a number of different workers for several series of related compounds (21-25). Quenching is relatively efficient and it is generally believed that the  $O_2(^1\Sigma_g^+)$  is deactivated to the  $O_2(^1\Delta_g)$  state.  $O_2(^1\Sigma_g^+)$  quenching is of little interest here and has been extensively reviewed in the literature (15,26).

In contrast to  $O_2(^1\Sigma_g^+)$ , the quenching of  $O_2(^1\Delta_g)$  is found to be particularly slow with rate constants often many orders of magnitude less than those for  $O_2(^1\Sigma_g^+)$  (2). A list of some of the more important rate constants that have been obtained in the gas phase is given in Table 3 (22,27-30). Kearns (31) has shown that there is a good correlation between the quenching rate constant and the overlap of the infrared vibrational bands of the quencher with the  $1.27 \mu$   $O_2(^1\Delta_g)$  emission band. He explains this by an energy transfer process of the  $O_2(^1\Delta_g)$  energy to the vibrational levels of the quencher. This process, unfortunately, cannot explain all the quenching data and there appears to be another more efficient quenching process responsible for the rapid deactivation of the  $O_2(^1\Delta_g)$  by amines (28) and sulphides (32). Ogryzlo (33) has correlated the rates of these processes with the ionization potentials of the related compounds and has suggested the involvement of a charge-transfer complex in the initial quenching interaction.

#### Reaction of Singlet Oxygen with Olefins

The reaction between singlet oxygen and various substituted olefins has become one of the most intensively studied areas of singlet oxygen chemistry over the last few years (15,34,35). The process involves attack of the singlet oxygen on the olefinic double bond, followed by rearrangement of the molecule and transfer of the allylic proton to produce the  $\alpha,\beta$ -unsaturated products:-

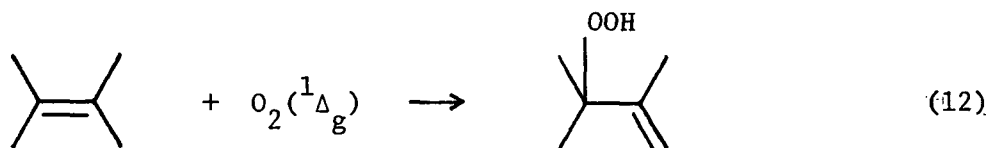
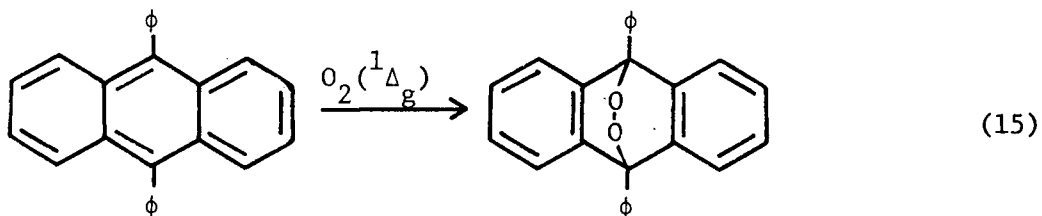
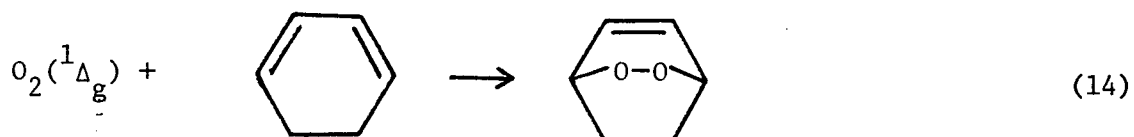
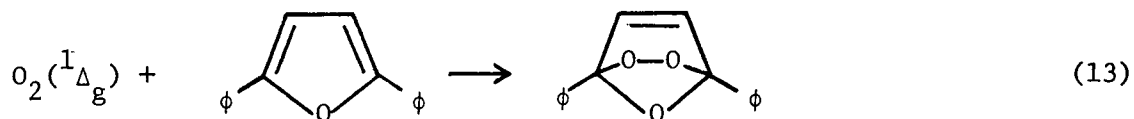


Table 3. The quenching efficiencies of  $O_2(^1\Delta_g)$  by different compounds.

Quencher	Rate litres mole <sup>-1</sup> sec <sup>-1</sup>	Reference
Oxygen $O_2$	$1.4 \times 10^3$	30
Nitrogen $N_2$	$4 \times 10^1$	30
Argon Ar	$1.2 \times 10^2$	30
Methane $CH_4$	$8.4 \times 10^2$	22
Propane $C_3H_8$	$1.4 \times 10^3$	22
Ethylene $C_2H_4$	$1.1 \times 10^3$	32
Propylene $C_3H_6$	$1.3 \times 10^3$	32
Butene-1 $C_4H_8$	$1.4 \times 10^3$	32
Pentene-1 $C_5H_{10}$	$1.9 \times 10^3$	32
Trimethylamine $N(CH_3)_3$	$1.9 \times 10^6$	28
Dimethylamine $NH(CH_3)_2$	$5.6 \times 10^4$	28
Methylamine $NH_2CH_3$	$8 \times 10^3$	28
Ammonia $NH_3$	$4.2 \times 10^3$	22
Methyl mercaptan $SHCH_3$	$2.3 \times 10^3$	27
Dimethyl sulphide $S(CH_3)_2$	$1.6 \times 10^5$	27

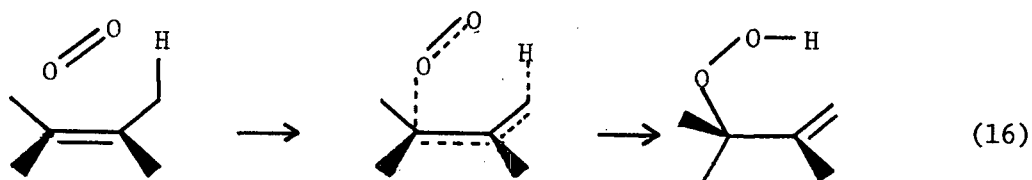
It has been found empirically that the reactivity of a particular olefin is largely governed by the individual character of the substituent groups adjacent to the unsaturated carbon atoms (16). Thus the electron-donating substituents of the alkyl, alkoxy or amino derivatives, which produce a high electron density at the  $\pi$  bond, also provide the most reactive members of the series; and conversely, those compounds having electron-withdrawing substituents in these positions are generally found to be rather low in reactivity. The direction of this effect has been explained by a certain amount of electrophilic character in the attacking  $O_2(^1\Delta_g)$  molecule.

In the special case of the conjugated cyclic dienes, the reaction is slightly different in that addition of the singlet oxygen occurs in a Diels-Alder fashion to produce the endoperoxide product. For example:-



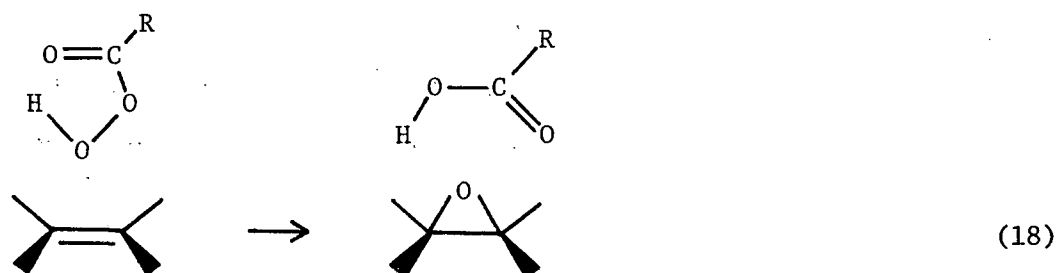
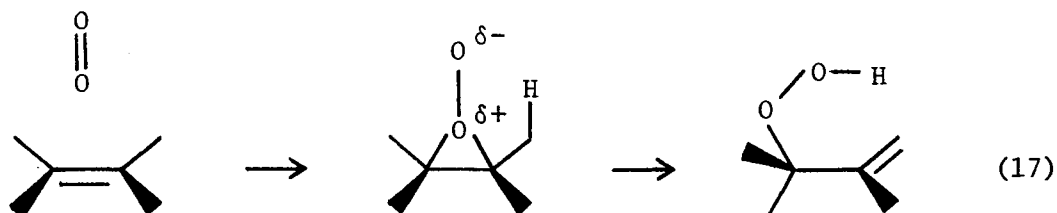
The effect of substituents on these reactions is analogous to that in reaction (12), in that a high reactivity is obtained with electron-donating groups in the 1,4 positions of the  $\pi$  electron system.

Both of these reactions have been well treated in the literature (34-39), although the majority of the discussion has been directed at the less familiar hydroperoxide reaction, for which three possible mechanisms have been seriously considered. The first and most popular of these - the 'ene' mechanism - was originally proposed by Nickon (40) and requires a concerted process involving the simultaneous addition of oxygen and abstraction of hydrogen via a six-membered transition state:-

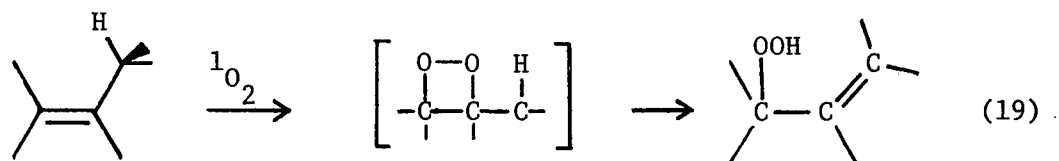


Certain characteristic features of this reaction, namely the *cis* relationship between the transferring hydrogen and the reacting oxygen, the lack of Markownikov effect on the product distribution and the apparent absence of any appreciable solvent influence on the rate, are all easily explained by this mechanism (36). Further support is provided by a detailed discussion of the stereochemical implications of the concerted addition to stereospecific compounds, particularly limonene, carene (38) and certain steroidal derivatives (40,41). The two other mechanisms that have been proposed for this reaction involve either a dioxetane or perepoxide intermediate and are found to explain the

substitution, solvent and stereochemical effects in a similar manner to the 'ene' mechanism (15,42). One particular piece of evidence in favour of a perepoxide intermediate is that the similarity between the substituent effect in the oxidation of olefins by peracids or by singlet oxygen can be explained by a similarity in the two mechanisms:-

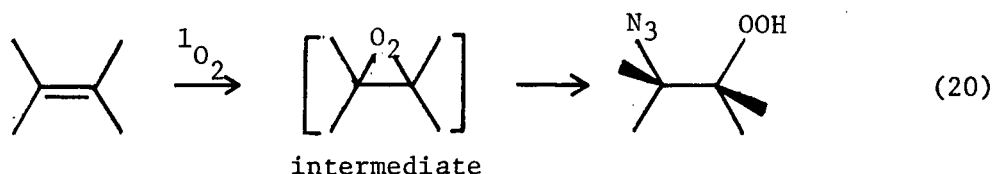


The major reason for the proposal of the dioxetane mechanism was to explain the formation of carbonyl products in the reaction of a variety of compounds, some of which did not contain an allylic hydrogen atom (48):-



Of these three possibilities, it was the 'ene' mechanism that was generally favoured until about 1969. At that time, Fenical, Kearns

and Radlick published a paper (44) showing seemingly irrefutable evidence against this mechanism which consisted of the formation and separation of an azidohydroperoxide product in the usual 2,3-dimethyl butene-2-hydroperoxide synthesis using the hydrogen peroxide decomposition method (Equation (9)) in the presence of the  $N_3^-$  ion:-



The formation of the azidohydroperoxide implied the existence of an intermediate in the reaction, a situation which was in direct contradiction to the point of view of the 'ene' mechanism. To support this finding, Kearns published a number of theoretical arguments (15, 42,45) favouring the existence of both the dioxetane and perepoxide intermediates, of which the first was neatly answered by Kopecky (46) who demonstrated that the 2,3-dimethyl butene-2-dioxetane adduct decomposed to produce acetone rather than the predicted allylic hydroperoxide product. This eliminated the dioxetane mechanism.

Finally, a more detailed investigation of the azide reaction by Foote, Fujimoto and Chang (47) strongly questioned the evidence of Kearns and suggested that the azidohydroperoxide product resulted from a side-reaction instead of the supposed attack on an intermediate.

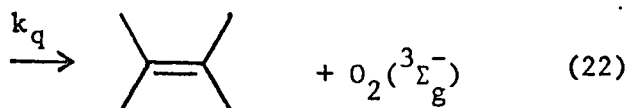
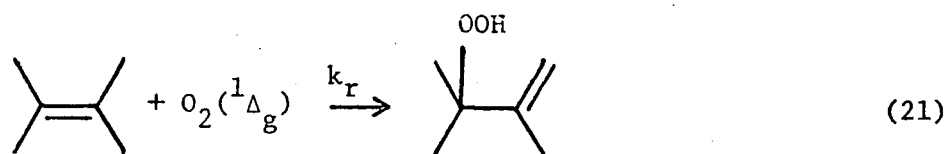
A recent suggestion by R.H. Young (48,49) is that the  $O_2(^1\Delta_g)$  forms a partial charge-transfer complex with the olefin before undergoing an 'ene'-type rearrangement to form the hydroperoxide. This is analogous

to the suggested intermediate in the reaction of a dienophile with a conjugated diene in a normal Diels-Alder addition reaction. The validity of this suggestion, however, is difficult to determine experimentally and has not been discussed to any extent by other workers.

### Gas Phase Reaction Studies

The kinetic investigation of the reactions of singlet oxygen with olefins in the gas phase has somewhat lagged behind the solution studies. This is not to say, however, that the state of confusion that has thrived in the solution work is in any way reduced in the gas-phase.

The competing, quenching and reaction processes of a typical olefin can be expressed as follows:-



where  $k_q$  and  $k_r$  represent the quenching and reaction rate constants, respectively. The kinetic analysis of these reactions can be treated in two distinct ways, depending on whether the decay of the  $\text{O}_2(^1\Delta_g)$  or the olefin is monitored. In the first of these, a large concentration of the reactant, R, is used in order to produce a pseudo-first order decay of the  $\text{O}_2(^1\Delta_g)$ . Thus:-

$$-\frac{d[\Delta_g^1]}{dt} = (k_r + k_q)[\Delta_g^1][R] \quad (23)$$

which gives on integration:-

$$\ln \frac{[\Delta_g^1]_0}{[\Delta_g^1]} = (k_r + k_q)[R]t \quad (24)$$

where the subscript refers to the  $O_2(\Delta_g^1)$  concentration at  $t = 0$ . In the second method the reverse procedure is adopted and the concentration of the  $O_2(\Delta_g^1)$  is made large compared with the olefin. Thus:-

$$-\frac{dR}{dt} = k_r[\Delta_g^1][R] \quad (25)$$

and integrating:-

$$\ln \frac{[R]_0}{[R]} = k_r[\Delta_g^1]t \quad (26)$$

Providing  $k_r$  and  $k_q$  are of a similar order of magnitude, these two methods are complementary in that both the quenching and reaction rate constants can be obtained by combining the two results.

In the original determination of these rate constants by Furukawa and Ogryzlo using the first of these methods,  $(k_r + k_q)$  was found to be linearly dependent on pressure, an effect which was later explained by the interference of a small quantity of atomic oxygen present as an impurity in the singlet oxygen stream. No pressure effect was found when they redetermined the rate constant for 2,3-dimethyl butene-2,

having removed the residual atomic oxygen by addition of a trace of  $\text{NO}_2$ , which reacts according to the fast reaction:-



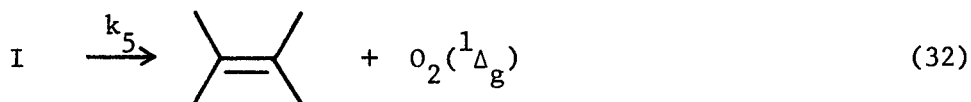
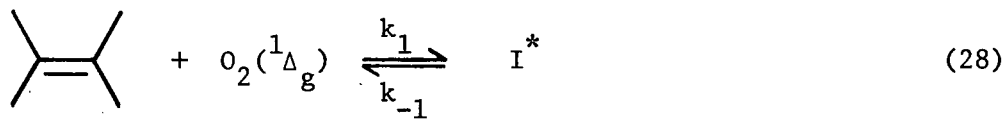
and thus removes the remaining oxygen atoms.

Ackerman, Pitts and Rosenthal have also made a determination of these rate constants for the series of straight chain mono-olefins. Unfortunately, even though their values are somewhat lower than those of Furukawa and Ogryzlo, they are no more reliable, as there is similarly no guarantee of the complete absence of atomic oxygen in their flowsystem.

The rate constants originally published by Herron and Huie (53) were also slightly in error and later reduced (54), presumably for the same reason. In their work, they measured  $k_r$  directly by following the decay of the olefin concentration using a mass spectrometer. By adding only a small quantity of the olefin, the  $\text{O}_2(^1\Delta_g)$  concentration remained effectively constant. Unfortunately, they were only able to measure the most rapid members of the series, making comparison with other results difficult.

Two other studies have been made on these reactions: The first was by Hollinden and Timmons (55) who determined the temperature dependence of the 2,3-dimethyl butene-2 and 2,5-dimethyl furan reactions using an ESR technique to follow the  $\text{O}_2(^1\Delta_g)$  concentration. They worked at fairly low pressures and it was found that their value of  $k_r$  for reaction with 2,3-dimethyl butene-2 agreed well with the results of the second study.

by Ackerman, Pitts and Steer (56) in which an inverse pressure effect was found. This was explained by the following mechanism:-



Both results must be treated with some suspicion, however, as no efforts were made to insure the complete removal of the atomic oxygen from the system. The values for each of these different determinations are shown in Table 4.

In the work presented here, a similar method to that employed by Herron and Huie was used to determine the temperature dependence of  $k_r$  for the series of olefins. Instead, however, of using the titration method for the determination of the  $\text{O}_2(^1\Delta_g)$  concentration (57), it was measured by observation of the 6340 Å band of the  $2(^1\Delta_g)$  dimole emission

Table 4. Rate constants for reaction of singlet oxygen with the olefins at room temperature.

Compound	Herron and Huie (54)	Furukawa and Ogryzlo (50)	Ackerman, Pitts and Rosenthal (56)
2,3-dimethyl pentene-2	$6.0 \times 10^5$	-	-
2,3-dimethyl butene-2 <sup>a</sup>	$8.6 \times 10^5$	$9.5 \times 10^5 /$ $7.5 \times 10^5$ <sup>b</sup>	$4.6 \times 10^5 /$ $1.2 \times 10^6$ <sup>c</sup>
2-methyl butene-2	$<1 \times 10^4$	$1 \times 10^5$	$1.4 \times 10^4$
cis-butene-2	$<1 \times 10^4$	$2.5 \times 10^4$	$1.3 \times 10^4$
trans-butene-2	$<1 \times 10^4$	$1 \times 10^4$	$3.0 \times 10^3$
1,2-dimethyl cyclopentene	$3.4 \times 10^5$	-	-
1-methyl cyclopentene	$1.3 \times 10^4$	$4 \times 10^5$	-
1,2-dimethyl cyclohexene	$3.4 \times 10^5$	-	-
1-methyl cyclohexene	-	$1 \times 10^4$	-
1,3-cyclohexadiene	$7.7 \times 10^5$	$2.3 \times 10^5$	-
cyclopentadiene	-	$8.8 \times 10^6$	-
2,5-dimethylfuran	$1.5 \times 10^7$	$2.8 \times 10^6$	$2.7 \times 10^7$

All rate constants given in units of litres mole<sup>-1</sup>sec<sup>-1</sup>.

<sup>b</sup> Hollinden and Timmons (51) room temperature value =  $1.2 \times 10^6$  litres mole<sup>-1</sup>sec<sup>-1</sup>.

<sup>c</sup> High (3 torr) pressure/low (1 torr) pressure.

with a suitable photomultiplier. The photomultiplier was then calibrated against an isothermal calorimeter. Herron and Huie's titration technique employs the fast reaction of 2,5-dimethylfuran with  $O_2(^1\Delta_g)$ , the decrease in the height of the observed mass peak being a direct measurement of the  $O_2(^1\Delta_g)$  concentration. The validity of this technique depends on the assumption that  $K_r \gg K_q$  for 2,5-dimethylfuran; some dispute over this point has arisen in the recent literature (58).

The lower limit to the rate constants measured by Herron and Huie at room temperature was overcome by running the experiments at higher temperatures. Rate constants were thus able to be measured down to the limit defined by the deactivation of singlet oxygen by the molecular oxygen carrier gas and the room temperature values obtained by extrapolation of the Arrhenius equation:-

$$k = A e^{-E_a/RT} \quad (33)$$

Thus if the data is plotted on a graph of  $\log(k_r)$  vs.  $1/T$ , the activation energy and preexponential A factors of the reaction can be simply obtained from the slope and intercept of the best straight line through the series of data points.

## EXPERIMENTAL

The apparatus used in each of the experiments described here was similar to that used in other conventional discharge flow systems except for the addition of a mass-spectrometer inlet leak sealed into the downstream end of the reaction tube. This arrangement allowed the continuous monitoring of the olefin and peroxide concentration in the vicinity of the sampling leak and thus provided a direct measure of the amount of olefin consumed in the specified reaction time.

### The Discharge-Flow System

The essential part of the apparatus used in the discharge flow technique is a uniform flow tube with a controlled gas inlet at one end and a rapid pumping system at the other. The gases are regulated to flow at a steady rate along the tube such that the time taken to flow from the inlet to the observation points can be accurately determined. By altering the relative positions of the reactant inlet and observation systems, or by changing the linear velocity of the gases along the tube, the time delay between these points can be varied over a considerable range, the only limitation being that the flowrate must be large compared with the diffusion rate through the gas.

A diagram of the apparatus used in the present work is shown in Fig. 3. The flow tube was constructed out of Pyrex glass and was approximately

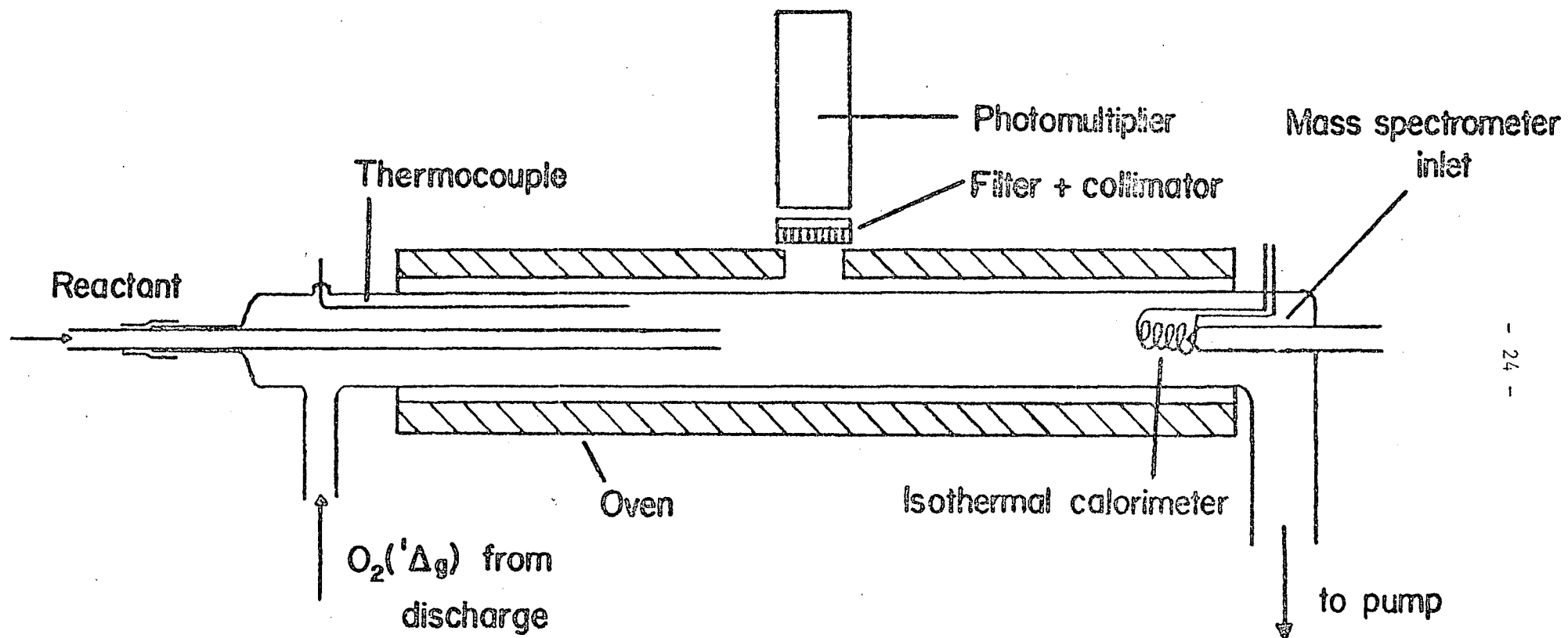


Figure 3. A diagram of the flowtube used in this work.

100 cm. long and 4.90 cm. in diameter. Flowrates, determined by collecting the quantity of gas passing through the system in a given time, were typically  $70 \text{ cm. sec}^{-1}$  or  $1 \times 10^{-4} \text{ mole. sec}^{-1}$  at a pressure of 2.50 torr within the reaction tube. Pressure was measured with a McLeod gauge which was found to be better suited for this work than the Pirani gauge used in the initial evacuation and leak testing stages.

The reactant olefin was added to the flow system through an Edward's needle valve backed by a 20 litre storage bulb, an arrangement which maintained the flow at a sufficiently constant level throughout an entire run. Some initial experiments which were performed in order to check the linearity of the reactant decay, employed a variable inlet which was moveable along the length of the tube. This is illustrated in Fig. 3. In the temperature dependence studies this inlet was replaced by a fixed inlet situated 85.0 cm upstream of the mass-spectrometer sampling leak. The flow tube was heated by an oven constructed of Chromel heating wire held in asbestos cloth surrounding several layers of aluminum foil, and insulated with a sheet of glass fibre wrapped around the outside of the tube. By controlling the current passing through the wire with a rheostat, the temperature of the tube could be varied and maintained at any value between room temperature and  $200^{\circ}\text{C}$ . A copper-constantan thermocouple with the junction covered with epoxy-resin to decrease the possibility of heating by deactivation of the singlet oxygen on the metal, was used to measure the temperature of the gas in the oven and was positioned in the tube as shown in Fig. 3. The potential difference across this thermocouple was displayed on a high impedance 10 mV strip chart recorder which was calibrated directly against a conventional laboratory thermometer in a series of heated baths.

A check was made of the uniformity in the temperature along the tube by replacing the variable reactant inlet by a thermocouple probe which could be moved along the length of the tube. It was found to be constant to within  $\sim 5\%$ .

### The Microwave Discharge

The oxygen discharge was maintained by a continuous source of 2450 MHz microwave power from an Electromedical Supplies "Microtron" generator supplied to the gas through a 214L 1/4 wave cavity which, by tuning to resonance, was found to produce a steadier discharge as well as minimizing the destructive interference with power reflected back along the leads. This concentration of power inside the cavity produced some rather high temperatures which necessitated the use of a quartz flow tube in the region of the discharge. Stray light was eliminated by passing the gas through a series of light traps before admitting it into the flow tube, and by covering the whole discharge area as well as the light traps in the flat black paint.

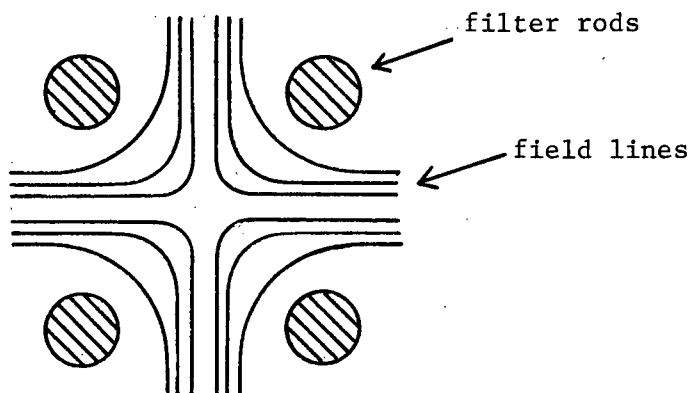
The atomic oxygen was removed from the discharge products by distilling a little mercury through the cavity to form a surface of mercuric oxide on the walls of the tube. It was found that if the mercury was placed near the discharge, it could be maintained at a sufficient temperature to be effective by simply altering the position of the cavity along the tube. Any traces of atomic oxygen escaping the mercuric oxide surface were removed by allowing a small quantity of nitrogen dioxide to enter the gas stream before reaching the reaction zone. This removes the oxygen atoms by the fast reaction:-



A certain amount of care has to be taken in the addition of the  $NO_2$  to the system as it is found that a large flow results in the appearance of the  $NO_2$  continuum which interferes with the photometric measurement of the  $O_2(^1\Delta_g)$  concentration. The mechanism for the production of this continuum is not entirely understood but involves an energy pooling process of the  $NO_2$  and the singlet oxygen. The correct flow of  $NO_2$  was conveniently produced here by storing it as a liquid in a small bulb and regulating the outflow of the vapour above the liquid using a teflon needle valve. A certain amount of difficulty was experienced in trying to change the concentration of the singlet oxygen in the gas stream by altering the power of the discharge and it was found to be easier to simply divide the oxygen flow into the discharge so that a certain regulated percentage was diverted around the microwave cavity. By this means the singlet oxygen concentration could be varied by almost an order of magnitude.

#### The Mass Spectrometer

The mass spectrometer was a '1210A' model supplied by Electronic Associates Inc. of Palo Alto, California. It was of the quadrupole 'mass-filter' kind and depended upon the combined effects of two perpendicular oscillating electric fields for its mass selection properties. The electric fields are generated between opposite pairs of four cylindrical stainless steel rods aligned parallel to each other in a square arrangement which would appear in cross section as follows:-



By careful adjustment of the relative amplitudes of the DC and RF components of the electric field, it is possible to restrict passage through the filter to ions whose  $m/e$  ratio lies in a certain precisely defined range. Ions with a higher or lower  $m/e$  ratio follow unstable trajectories and either escape through the gaps in the filter or collide with the rods, becoming neutralized. The ions are produced by a conventional axially-mounted electron bombardment ion source and accelerated into the filter by an appropriate potential. They are detected by a 14-stage beryllium-copper secondary emission electron multiplier situated at the other end of the filter assembly. The instrument was divided into three separate sections: the quadrupole head itself with the ion source, filter rods, and electron multiplier mounted axially on a 6 inch bakeable flange; the radio frequency generating unit situated immediately behind the head assembly, and a control unit consisting of the power supplies for the ion source and electron multiplier as well as the DC ramp voltage generators which control the mass filter. This is shown diagrammatically in Fig. 4. The output current from the electron multiplier, which was generally in the

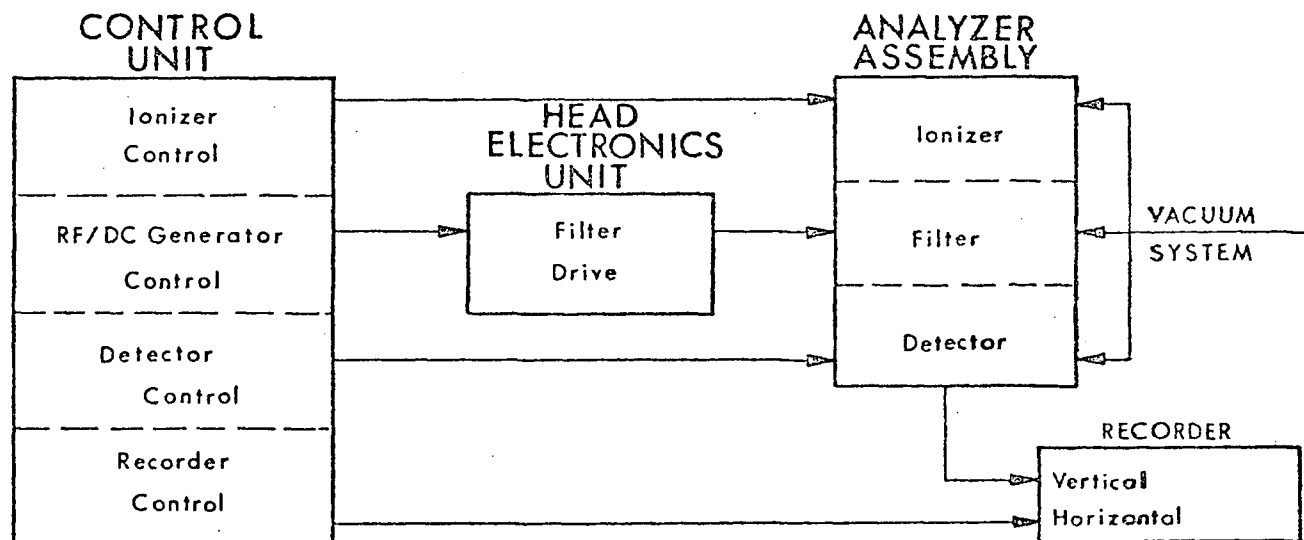


Figure 4. Schematic diagram of the electronics used to control the quadrupole mass spectrometer.

range of  $10^{-7}$  to  $10^{-10}$  amps with a first dynode voltage of -2900 volts, could either be connected directly into an oscilloscope or amplified and displayed on a strip chart recorder.

The controls on the instrument allowed the electron energy, resolution and accelerating voltage to be adjusted as well as the position and range of the mass sweep. A simple modification also allowed the instrument to 'sit' on the top of a mass peak and thus provided a means of continuously monitoring the change in a particular sample concentration. When used in this mode, it was necessary to adjust the resolution, electron and accelerating voltages for maximum signal and minimum overlap of neighbouring peaks, before disabling the mass sweep; one could then be certain that the instrument was being used in a precisely controlled and efficient manner. Operation of the instrument required a pressure of less than  $10^{-4}$  torr on the quadrupole head assembly. In order to maintain this pressure under the continuous inflow of gas from the rest of the apparatus, a rapid pumping arrangement was constructed, consisting of a 6 inch diameter CVC diffusion pump, in conjunction with a Welch 2-stage mechanical pump. The pumping and inlet arrangements are shown in Fig. 5. A vacuum of  $2 \times 10^{-7}$  torr which was obtainable in this system with the inlet leak closed, rose to about  $5 \times 10^{-6}$  torr when the inlet leak was opened to a pressure of 2.50 torr in the flow system. The quadrupole head was surrounded with heating wire embedded in several layers of asbestos cloth allowing this part of the vacuum system to be baked to a temperature of about  $200^{\circ}\text{C}$ . Although only a small decrease in pressure was obtained by this means, presumably because of the large surface areas of cold metal in the cold trap and

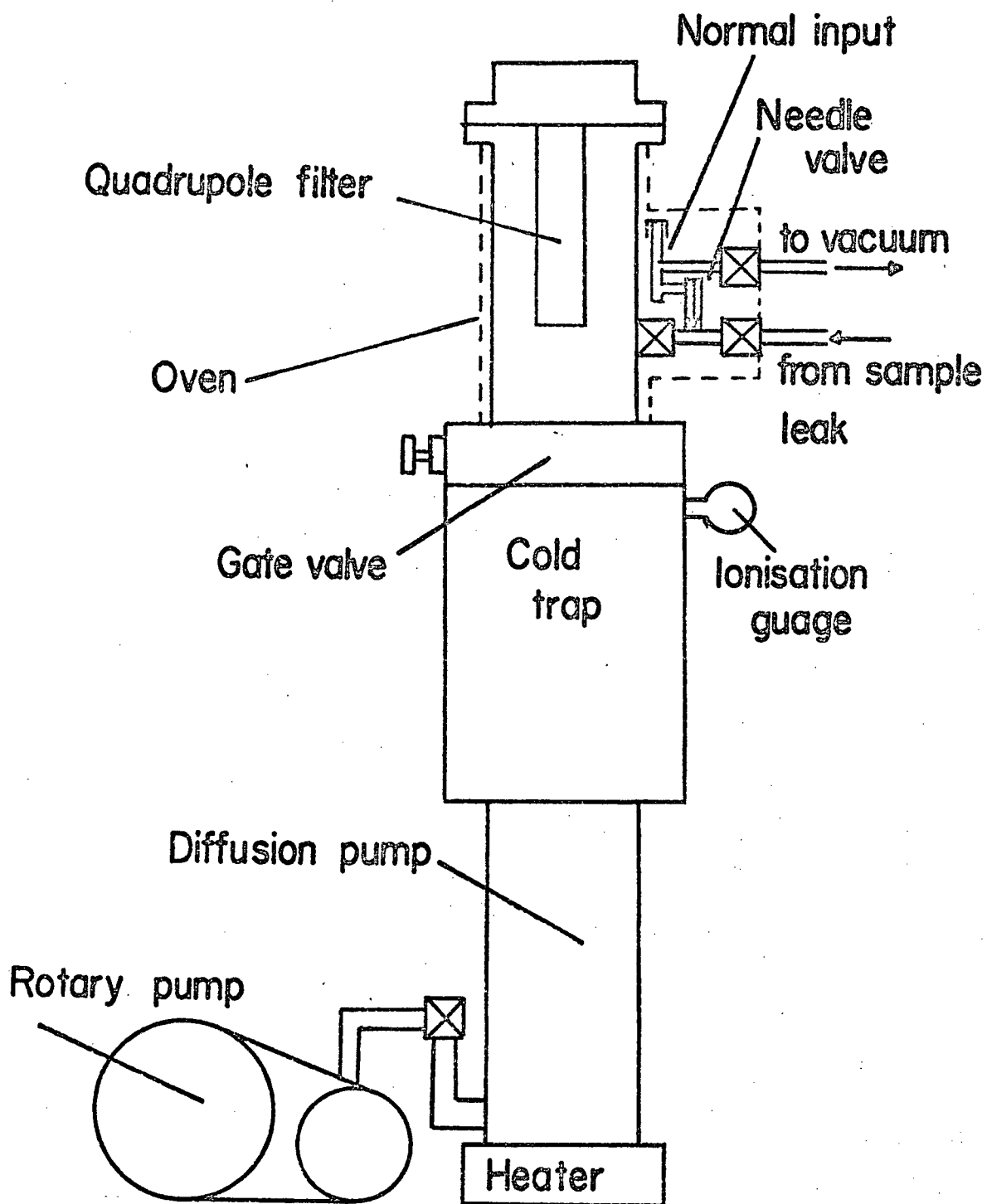


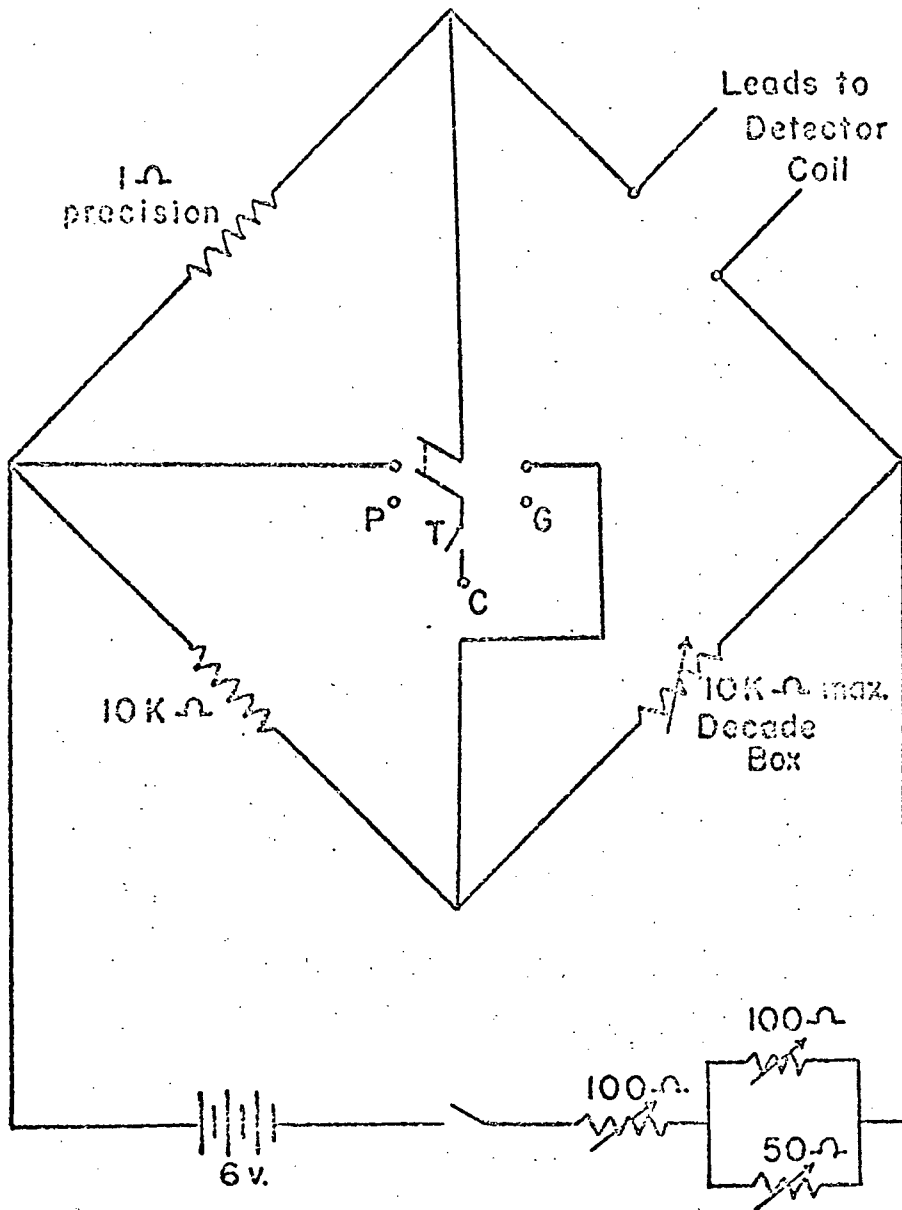
Figure 5. The mass spectrometer pumping arrangement.

gate valve, baking did serve to remove a substantial portion of the detectable background spectrum of the residual gases and was thus employed for several hours before each run. Even so, the CVC 'Convalex-10' polyphenol pump oil used in the diffusion pump produced a very low residual spectrum, in spite of the fact that a certain amount of 'cracking' was apparent after the instrument had been running for a while.

The mass spectrometer inlet leak was conveniently produced by sealing the end of a piece of 1 cm i.d. glass tubing, heating a small area with a fine flame and then pulling the glass out rapidly with a glass rod. The fine capillary produced was then broken off at the desired hole diameter. Other, more orthodox designs were tried, but found to be considerably more trouble to construct and set up, particularly with regard to obtaining the correct hole size. The inlet does admittedly suffer from a certain degree of fragility but can be protected by surrounding the tube with a stout cylindrical shield.

#### Determination of the $O_2(^1\Delta_g)$ Concentration

In order to calculate the rate constants for the individual olefins, it is necessary to determine the absolute value of the  $O_2(^1\Delta_g)$  concentration in the flow tube. Several methods are now known for doing this; none, however, is as reliable or as well tested as the isothermal calorimeter technique (59). This consists of measuring the energy gained when the  $O_2(^1\Delta_g)$  is deactivated on an electrically heated wire known as the detector. This energy causes heating of the detector, which is compensated by an appropriate decrease in the current through



P potentiometer terminal  
 C common  
 G galvanometer  
 T tapping key

Figure 6. The circuit of the isothermal calorimeter.

the wire, the difference providing an accurate measure of the  $O_2(^1\Delta_g)$  concentration. In practice the detector consists of a helically wound spiral of platinum wire, electroplated with cobalt. The circuit is shown in Fig. 6. In the absence of  $O_2(^1\Delta_g)$ , the bridge is balanced allowing the resistance,  $R$ , of the detector to be determined and the current,  $i_o$ , to be measured on a potentiometric strip chart recorder. The  $O_2(^1\Delta_g)$  is then produced by starting the discharge, and the bridge rebalanced by decreasing the current through the wire. Thus by equalizing  $R$  before and after the  $O_2(^1\Delta_g)$  addition, the temperature of the detector is maintained at a constant value. The current ( $i$ ) is again measured and the  $O_2(^1\Delta_g)$  flowrate obtained from the following equation:-

$$\frac{d[O_2(^1\Delta_g)]}{dt} = \frac{(i)^2 R}{K E} \quad (34)$$

where  $(i)^2 = i_o^2 - i^2$

$E$  = energy liberated per molecule (= 23 Kcals mole<sup>-1</sup> for  $O_2(^1\Delta_g)$ )

$K$  = 4.18 cal sec watt<sup>-1</sup>

The efficiency of the detector was checked by coating the walls of the flow tube downstream of the detector with a solution of violanthrone in n-buthyl phthalate. This compound is known to fluoresce strongly in the presence of singlet oxygen. No emission was seen in the present case. Further evidence of the total efficiency of the detector was provided by the fact that similar results were obtained when runs were repeated using a freshly plated calorimeter.

Although in theory the isothermal calorimeter could be used to determine the  $O_2(^1\Delta_g)$  concentration directly, in practice this was not possible as the surface of the detector gradually became 'poisoned' by the presence of the olefin, particularly at high temperature. To overcome this difficulty the  $O_2(^1\Delta_g)$  concentration was followed photometrically using the 6340 Å dimole emission band. The recorded signal was calibrated using a known concentration of  $O_2(^1\Delta_g)$  determined using a freshly plated isothermal calorimeter. The R.C.A. 7265 photomultiplier had an S20 response and was situated about halfway along the reaction tube (see Fig. 3) where it observed the  $O_2(^1\Delta_g)$  emission through an interference filter and a 15° 'honeycomb' collimator. The signal was amplified by a Keitley Micro-microammeter and displayed on a conventional strip chart recorder.

#### Chemicals

Oxygen	Matheson Extra Dry Grade
Nitrogen Dioxide	Matheson Co.
2-Methyl butene-2	Phillips 66 Co.
Cis-butene	Phillips 66 Co.
1-Methyl cyclohexene	Phillips 66 Co.
trans-Butene	Phillips 66 Co.
1,2-Dimethyl cyclohexene	Chemical Samples Co.
1,2-Dimethyl cyclopentene	Chemical Samples Co.
2,3-Dimethyl butene-2	Aldrich Chemical Co.
1-Methyl cyclopentene	Aldrich Chemical Co.
Cyclopentene	Aldrich Chemical Co.

Furan	Aldrich Chemical Co.
Cyclohexene	Eastman Kodak Co.
2-Methylfuran	Eastman Kodak Co.
Cyclohexadiene	Aldrich Chemical Co.
Cyclopentadiene	Produced by fractional distillation from dicyclopentadiene heated to 160°C. Dicyclopentadiene obtained from Velsicol Chemical Co.

All chemicals were used as supplied by the manufacturers, although a purity check was made on each of the compounds using gas chromatographic analysis. Even in the worst case of ~2% impurity, little interference with the observed rate constant would be expected as the reaction was followed using a major peak of the reactant mass spectrum.

## RESULTS

As mentioned earlier, the rate equation for the  $O_2(^1\Delta_g)$ -olefin reaction can be integrated to give the following expression:-

$$\ln(R_o/R) = k_r[^1\Delta_g]t \quad (25)$$

which is first order in R provided there is negligible consumption of the  $O_2(^1\Delta_g)$  during the course of the reaction. This situation is only true for small concentrations of the reactant R, such that  $[O_2(^1\Delta_g)] \gg [R]$ , as is the case in the present work. Equation (25) can thus be applied directly. In use a further simplification can be made: Since only the relative values of the reactant concentration are required, the magnitude of the output signal from the mass spectrometer can be substituted directly into equation (25), giving:-

$$\ln(H_o/H) = k_r[^1\Delta_g]t \quad (35)$$

where H represents the height of the reactant peak. The validity of this expression depends on the direct linearity between H and the reactant concentration and was checked by measuring the peak heights corresponding to known pressures of argon ( $m/e = 40$ ) in the flow tube, as shown in

Fig. 7. The rate constant can thus be conveniently obtained from the slope of the  $\log(H_0/H)$  vs. time plots.

The major limitation of this approach is that overlap between product and reactant mass spectra can cause an apparent increase in the reactant concentration monitored at a particular  $m/e$  value. The magnitude of this interference will obviously vary from peak to peak with the different fragmentation patterns, but can be expressed for an individual peak by a slight modification of equation (35):-

$$\ln\left[\frac{H_0}{H^* + n(H_0 - H^*)/(1+n)}\right] = k_r [^1\Delta_g]t \quad (36)$$

where  $H^*$  is the apparent peak height. The constant  $n$  serves to relate the signal observed for a unit concentration of product to that of the reactant. It depends on the  $m/e$  ratio used as well as the ionisation characteristics of the mass spectrometer.

By comparison of equations (35) and (36) it can be seen that for  $H^* \gg (H_0 - H^*)$  and  $n \ll 1$ , a good approximation will be obtained by letting  $H^* = H$  and assuming that equation (35) holds under these circumstances. It is thus necessary when setting up an experiment to be rather careful to choose a reactant peak for which  $n$  is small. In the present work the parent peak ( $M^+$ ) was used to follow the reactant concentration in all cases. The justification for this is three-fold:-

(1) The mass spectra for the most reactive members of each series of compounds for which a substantial amount of reaction could be observed, did not contain any large peaks due to major product fragments at the mass number of the parent peak. The slower members of the series

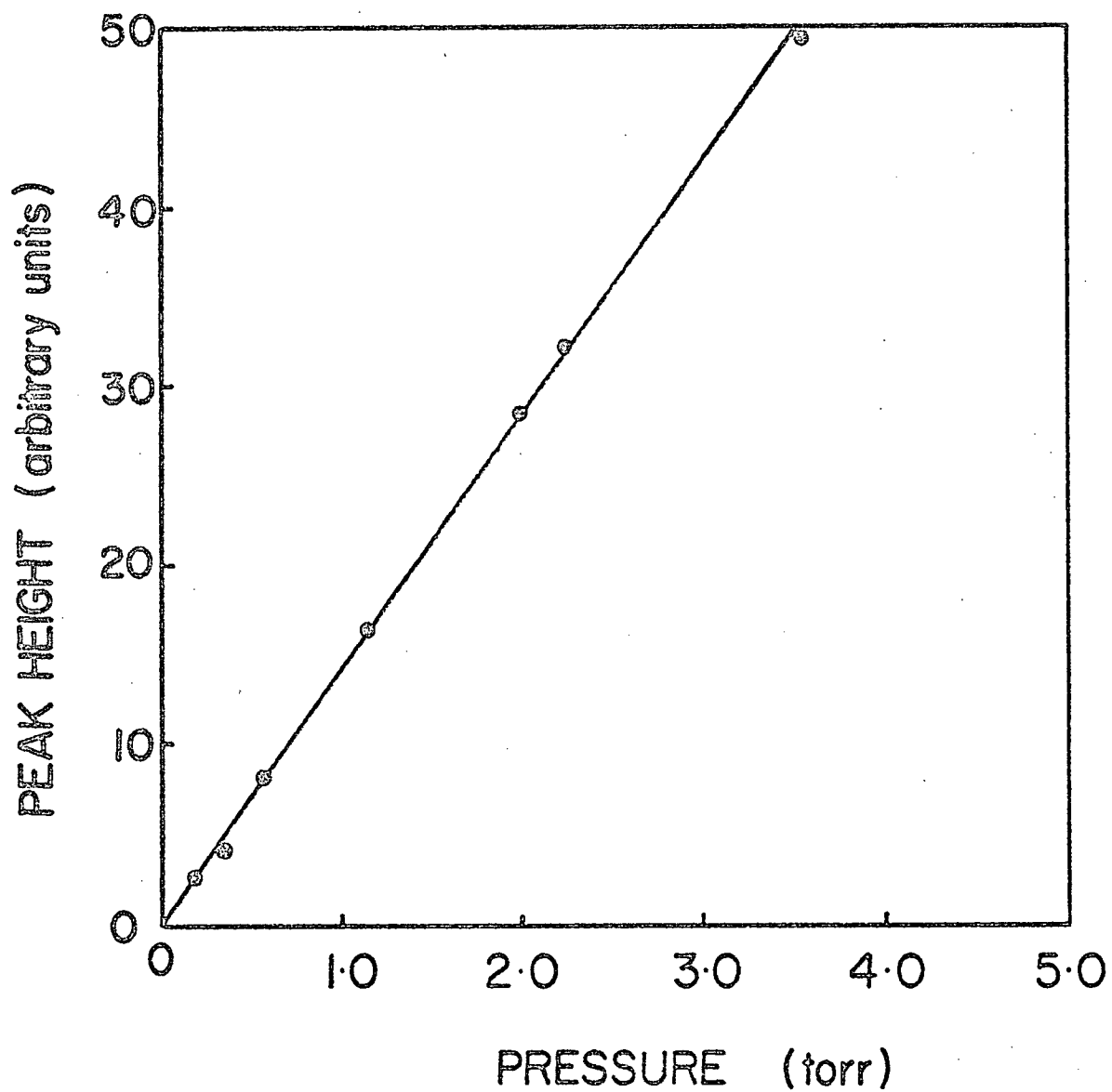


Figure 7. The relationship between the peak height observed in the mass spectrometer and the partial pressure within the flowtube for argon.

would not be expected to diverge from this general trend to any great extent.

(2) Plots of  $\log(H_O/H)$  vs. time for all compounds showed a straight line first-order dependence as is illustrated in Fig. 8 for the faster members of each series. Any interference due to product peak appearance would be expected to show up as a curvature of these lines, with an observable decrease in the slope at large  $t$  indicating a significant contribution from the  $n(H_O-H^*)/(1+n)$  term.

(3) By altering the  $O_2(^1\Delta_g)$  concentration in the tube,  $(H_O-H^*)$  was kept at a small value compared with  $H^*$ . Thus, provided  $n$  was not extraordinarily large, the  $n(H_O-H^*)/(1+n)$  term in equation (36) would have a negligible contribution to the logarithmic term and so to  $K_r$ . Values of about  $(0.15)H_O$  were regarded as being ideal for the magnitude of the  $(H_O-H^*)$  term in that they provided a good compromise between a small product contribution on the one hand and a good discrimination from the signal noise on the other.

Further corroboration of these assumptions is provided by the work of Herron and Huie (54) who not only demonstrate a similar linearity of the  $\log(H_O/H)$  vs. time plots but also in the plots of product formed vs. reactant consumed for 2,3-dimethylbutene-2 and 2,5-dimethylfuran.

#### The Temperature Dependence of the $O_2(^1\Delta_g)$ -Olefin Reaction

The temperature dependence of the rate constants for the series of olefins studied here was obtained at about 2.50 torr using a fixed inlet situated 85 cm upstream of the mass spectrometer sampling leak. The results of these experiments are listed in Tables 5 to 17. The values that are quoted represent the mean of several determinations of

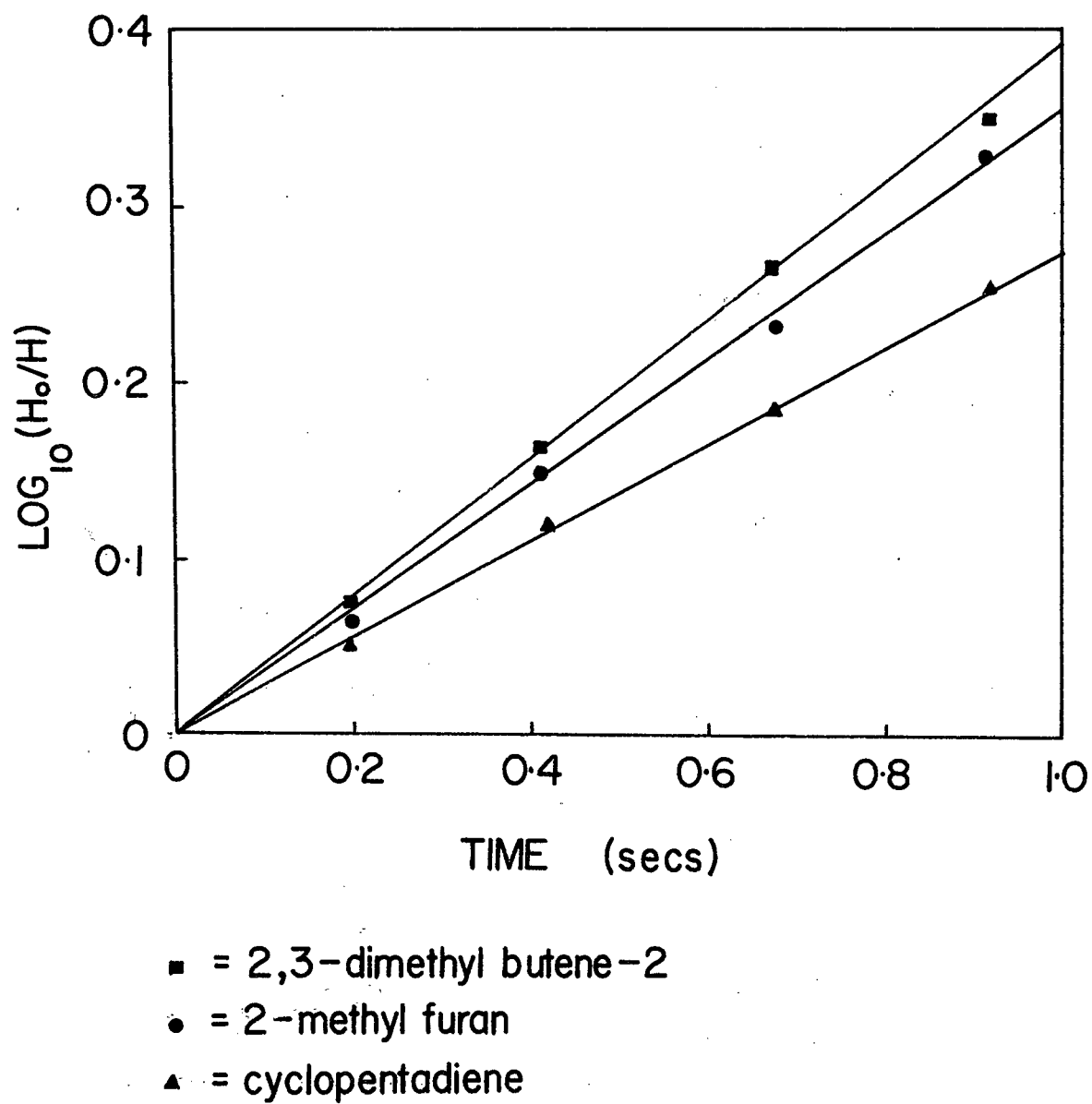


Figure 8. Plots of  $\log(H_0/H)$  vs. time at  $\sim 150^\circ\text{C}$ .

Table 5. The data used to calculate the rate constants for 2,3-dimethyl butene-2 at each temperature.

Temperature (°K <sup>-1</sup> )	Flowrate cm/sec	H/H <sub>0</sub>	O <sub>2</sub> ( <sup>1</sup> Δ <sub>g</sub> ) concentration (moles litre <sup>-1</sup> ) x 10 <sup>-7</sup>	Rate constant (litres mole <sup>-1</sup> sec <sup>-1</sup> ) x 10 <sup>5</sup>
297	68.99	0.484	9.84	5.94
297	67.60	0.479	10.90	6.01
328	76.20	0.456	7.69	9.17
337	76.70	0.421	7.92	11.0
359	83.39	0.408	6.20	14.2
370	84.21	0.424	5.61	16.9
394	91.52	0.393	4.69	21.6
397	90.36	0.426	4.16	24.0
422	98.03	0.396	3.77	28.6
426	96.96	0.457	3.12	32.2

Table 6. The data used to calculate the rate constants for  
2-methyl butene-2 at each temperature.

Temperature (°K <sup>-1</sup> )	Flowrate cm/sec	H/H <sub>0</sub>	O <sub>2</sub> ( <sup>1</sup> Δ <sub>g</sub> ) concentration (moles litre <sup>-1</sup> ) x 10 <sup>-7</sup>	Rate constant (litres mole <sup>-1</sup> sec <sup>-1</sup> ) x 10 <sup>4</sup>
321	81.09	0.915	16.5	5.12
343	86.65	0.880	14.6	8.90
371	93.72	0.850	11.6	15.4
392	98.90	0.851	9.84	19.1
417	105.2	0.836	7.95	27.8
444	112.2	0.804	6.49	44.5
454	114.7	0.808	5.81	49.6

Table 7. The data used to calculate the rate constants for cis butene-2 at each temperature.

Temperature (°K <sup>-1</sup> )	Flowrate cm/sec	H/H <sub>o</sub>	O <sub>2</sub> ( <sup>1</sup> Δ <sub>g</sub> ) concentration (moles litre <sup>-1</sup> ) x 10 <sup>-7</sup>	Rate constant (litres mole <sup>-1</sup> sec <sup>-1</sup> ) x 10 <sup>4</sup>
381	92.01	0.983	12.7	2.49
391	94.42	0.970	10.8	3.15
407	98.93	0.966	9.83	4.09
422	102.6	0.960	9.02	5.54
440	106.9	0.946	8.47	8.18
455	109.9	0.940	7.62	10.4
467	113.5	0.936	7.19	12.3
491	119.3	0.940	5.43	16.0

Table 8. The data used to calculate the rate constants for trans butene-2 at each temperature.

Temperature (°K <sup>-1</sup> )	Flowrate cm/sec	H/H <sub>o</sub>	O <sub>2</sub> ( <sup>1</sup> Δ <sub>g</sub> ) concentration (moles litre <sup>-1</sup> ) x 10 <sup>-7</sup>	Rate constant (litres mole <sup>-1</sup> sec <sup>-1</sup> ) x 10 <sup>4</sup>
405	96.16	0.982	7.74	2.31
420	99.73	0.979	6.98	3.12
426	101.1	0.977	6.53	3.73
437	103.8	0.976	5.66	4.66
449	106.6	0.972	5.34	5.90
457	108.5	0.972	4.64	6.81
470	111.6	0.976	3.97	7.93
487	115.6	0.970	3.37	10.6

Table 9. The data used to calculate the rate constants for  
1,2-dimethyl cyclohexene at each temperature.

Temperature (°K <sup>-1</sup> )	Flowrate cm/sec	H/H <sub>0</sub>	O <sub>2</sub> ( <sup>1</sup> Δ <sub>g</sub> ) concentration (moles litre <sup>-1</sup> ) x 10 <sup>-7</sup>	Rate constant (litres mole <sup>-1</sup> sec <sup>-1</sup> ) x 10 <sup>5</sup>
297	69.96	0.759	7.51	3.02
324	76.32	0.682	6.76	5.09
357	84.09	0.571	5.92	9.36
393	92.57	0.500	4.92	15.4
414	97.52	0.438	4.60	20.7
444	104.6	0.427	4.08	25.7
466	109.8	0.354	3.65	36.7

Table 10. The data used to calculate the rate constants for  
1-methyl cyclohexene at each temperature.

Temperature (°K <sup>-1</sup> )	Flowrate cm/sec	H/H <sub>0</sub>	O <sub>2</sub> ( <sup>1</sup> Δ <sub>g</sub> ) concentration (moles litre <sup>-1</sup> ) x 10 <sup>-6</sup>	Rate constant (litres mole <sup>-1</sup> sec <sup>-1</sup> ) x 10 <sup>4</sup>
406	97.97	0.966	1.80	2.16
409	95.92	0.925	4.01	32.27
423	102.1	0.962	1.59	3.11
427	100.1	0.897	3.75	3.50
440	106.2	0.951	1.44	4.26
446	104.6	0.877	3.45	4.80
460	107.9	0.849	3.27	6.55
463	111.7	0.932	1.27	7.01
480	112.6	0.844	2.90	8.57
484	116.8	0.921	1.11	9.91

Table 11. The data used to calculate the rate constants for  
1,2-dimethyl cyclopentene at each temperature.

Temperature (°K <sup>-1</sup> )	Flowrate cm/sec	H/H <sub>O</sub>	O <sub>2</sub> ( <sup>1</sup> Δ <sub>g</sub> ) concentration (moles litre <sup>-1</sup> ) x 10 <sup>-7</sup>	Rate constant (litres mole <sup>-1</sup> sec <sup>-1</sup> ) x 10 <sup>5</sup>
308	72.23	0.647	8.91	4.15
344	80.67	0.474	6.70	7.85
383	89.82	0.549	4.70	13.5
419	98.16	0.521	3.24	23.3
453	106.2	0.514	2.45	34.0

Table 12. The data used to calculate the rate constants for  
1-methyl cyclopentene at each temperature.

Temperature (°K <sup>-1</sup> )	Flowrate cm/sec	H/H <sub>o</sub>	O <sub>2</sub> ( <sup>1</sup> Δ <sub>g</sub> ) concentration (moles litre <sup>-1</sup> ) x 10 <sup>-6</sup>	Rate constant (litres mole <sup>-1</sup> sec <sup>-1</sup> ) x 10 <sup>4</sup>
299	69.73	0.942	3.90	1.25
346	80.69	0.879	2.76	4.45
402	93.75	0.758	1.86	16.4
437	101.9	0.746	1.44	31.2
463	108.0	0.720	1.01	41.3

Table 13. The data used to calculate the rate constants for cyclopentene at each temperature.

Temperature (°K <sup>-1</sup> )	Flowrate cm/sec	H/H <sub>0</sub>	O <sub>2</sub> ( <sup>1</sup> Δ <sub>g</sub> ) concentration (moles litre <sup>-1</sup> ) x 10 <sup>-6</sup>	Rate constant (litres mole <sup>-1</sup> sec <sup>-1</sup> ) x 10 <sup>4</sup>
386	92.74	0.974	1.89	1.55
404	97.06	0.968	1.59	2.37
418	100.4	0.959	1.43	3.44
435	104.5	0.950	1.46	4.31
453	108.8	0.944	1.30	5.65
465	111.7	0.925	1.18	8.71
478	114.8	0.923	1.08	10.1

Table 14. The data used to calculate the rate constants for furan at each temperature.

Temperature (°K <sup>-1</sup> )	Flowrate cm/sec	H/H <sub>o</sub>	O <sub>2</sub> ( <sup>1</sup> Δ <sub>g</sub> ) concentration (moles litre <sup>-1</sup> ) x 10 <sup>-7</sup>	Rate constants (litres mole <sup>-1</sup> sec <sup>-1</sup> ) x 10 <sup>4</sup>
324	76.68	0.929	15.5	4.33
341	80.71	0.910	14.0	6.36
359	84.97	0.882	13.4	9.33
390	92.30	0.839	11.6	16.4
418	98.93	0.793	9.84	27.4
449	106.3	0.769	7.93	41.4

Table 15. The data used to calculate the rate constants for  
2-methylfuran at each temperature.

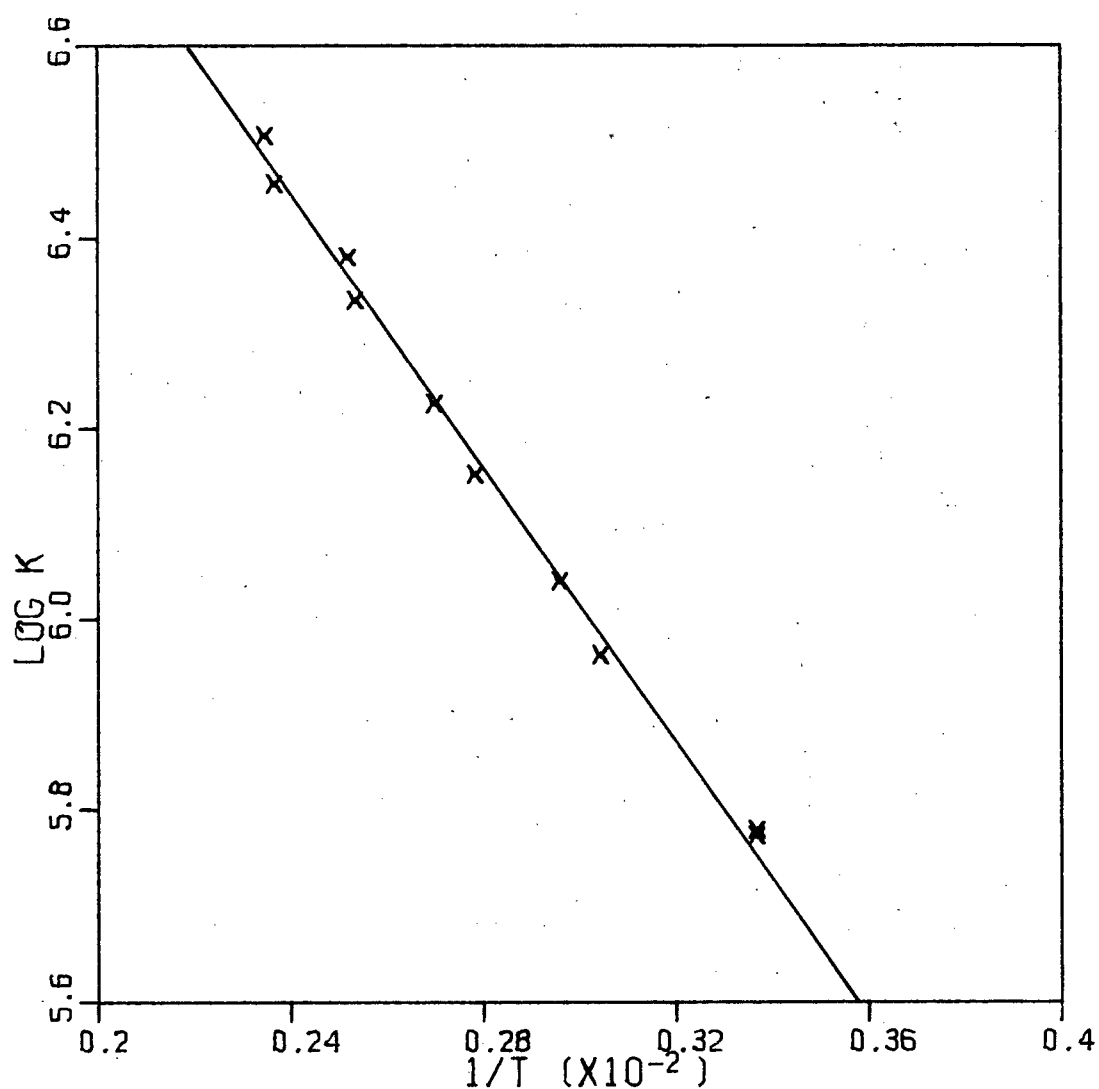
Temperature (°K <sup>-1</sup> )	Flowrate cm/sec	H/H <sub>o</sub>	O <sub>2</sub> ( <sup>1</sup> Δ <sub>g</sub> ) concentration (moles litre <sup>-1</sup> ) x 10 <sup>-7</sup>	Rate constant (litres mole <sup>-1</sup> sec <sup>-1</sup> ) x 10 <sup>5</sup>
297	73.52	0.236	35.7	3.50
340	84.17	0.117	27.4	7.75
389	96.30	0.056	22.5	1.45
430	106.5	0.052	15.4	2.40
477	118.1	0.105	7.86	3.99

Table 16. The data used to calculate the rate constants for cyclopentadiene at each temperature.

Temperature (°K <sup>-1</sup> )	Flowrate cm/sec	H/H <sub>o</sub>	O <sub>2</sub> ( <sup>1</sup> Δ <sub>g</sub> ) concentration (moles litre <sup>-1</sup> ) x 10 <sup>-7</sup>	Rate constant (litres mole <sup>-1</sup> sec <sup>-1</sup> ) x 10 <sup>5</sup>
303	72.48	0.232	6.13	3.77
351	83.96	0.106	10.1	9.75
382	91.38	0.071	19.8	14.4
428	102.4	0.147	22.8	23.0
473	113.1	0.150	33.1	41.2

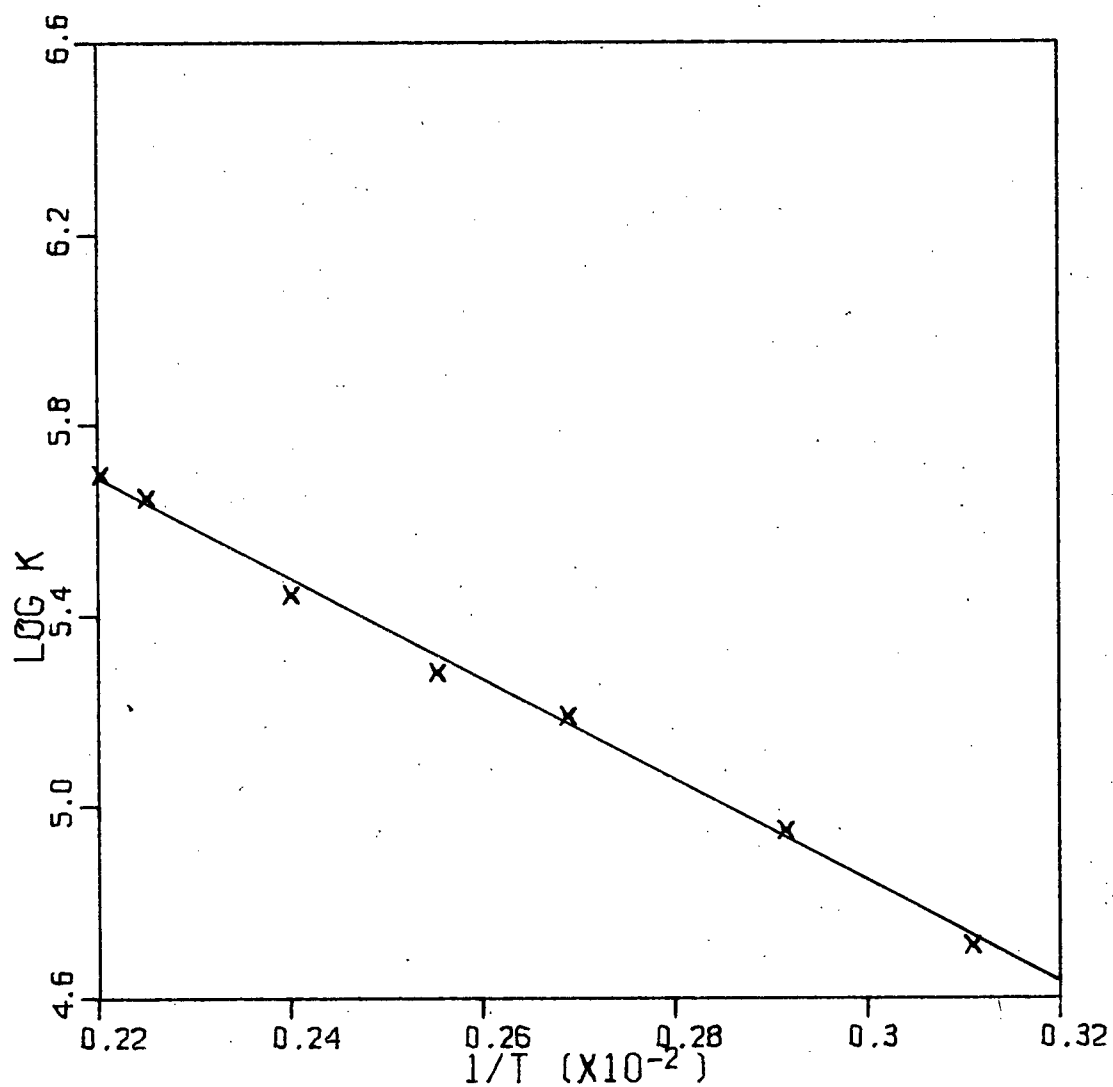
Table 17. The data used to calculate the rate constants for  
1,3-cyclohexadiene at each temperature.

Temperature (°K <sup>-1</sup> )	Flowrate cm/sec	H/H <sub>o</sub>	O <sub>2</sub> ( <sup>1</sup> Δ <sub>g</sub> ) concentration (moles litre <sup>-1</sup> ) x 10 <sup>-6</sup>	Rate constant (litres mole <sup>-1</sup> sec <sup>-1</sup> ) x 10 <sup>4</sup>
298	71.22	0.915	5.09	1.46
299	71.20	0.900	4.80	1.83
334	79.82	0.843	4.07	3.95
347	82.64	0.800	3.99	5.43
368	87.95	0.756	3.42	8.46
396	94.30	0.643	3.17	15.5
413	98.70	0.592	2.85	21.4
450	107.5	0.509	2.41	35.6



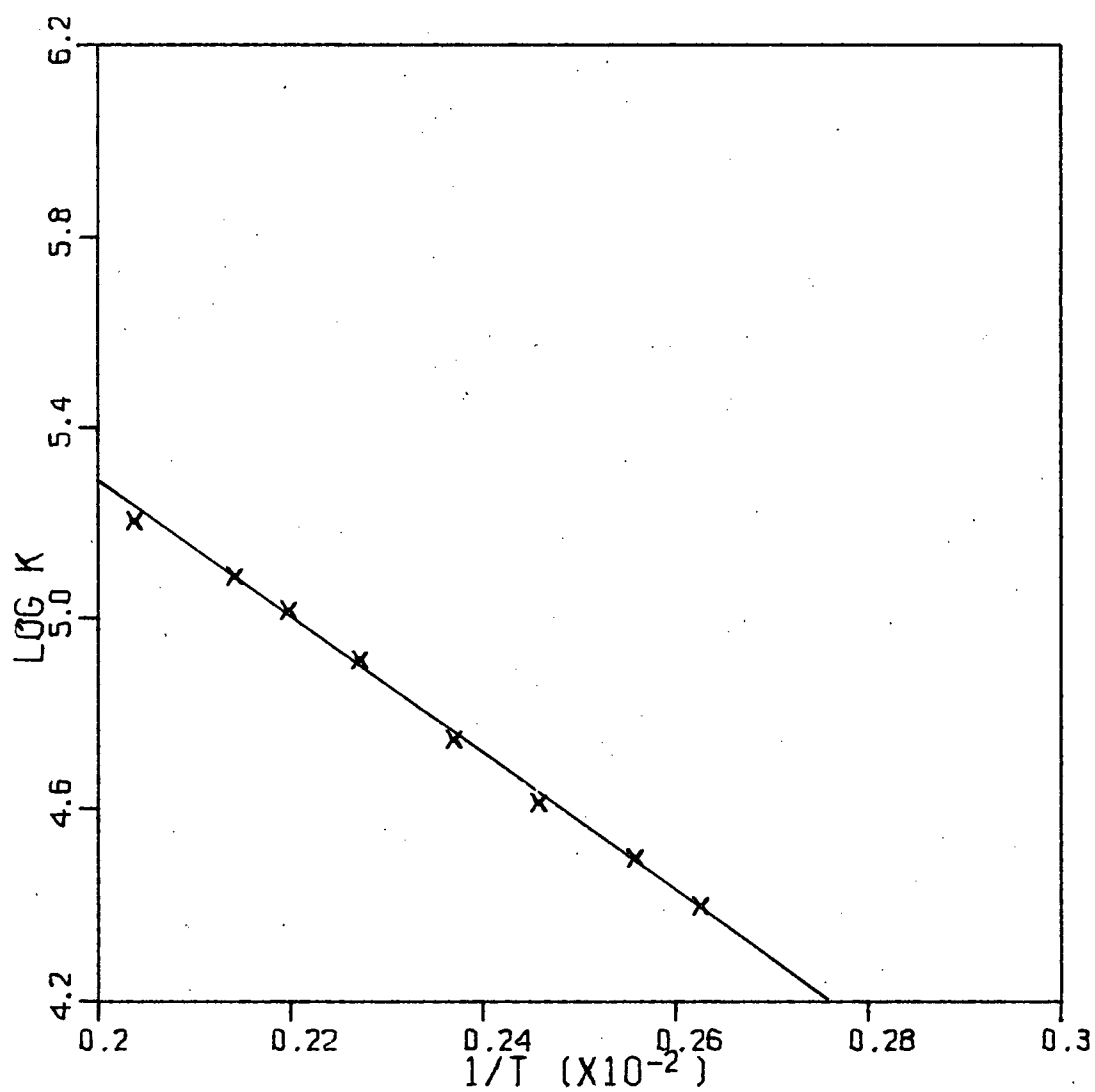
## 2.3 DIMETHYL BUTENE-2

Figure 9. Arrhenius plot



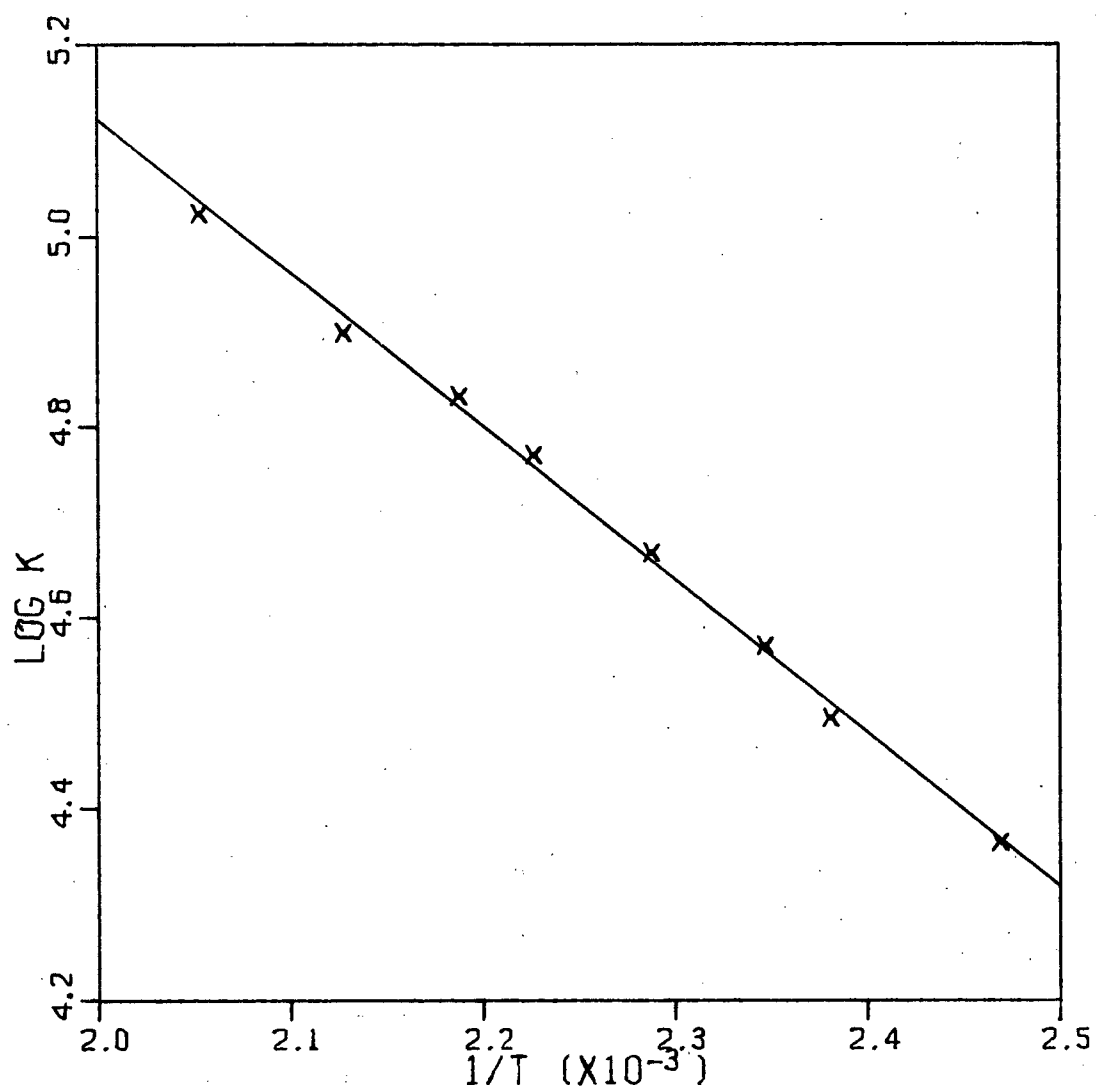
2 METHYL BUTENE-2

Figure 10. Arrhenius plot



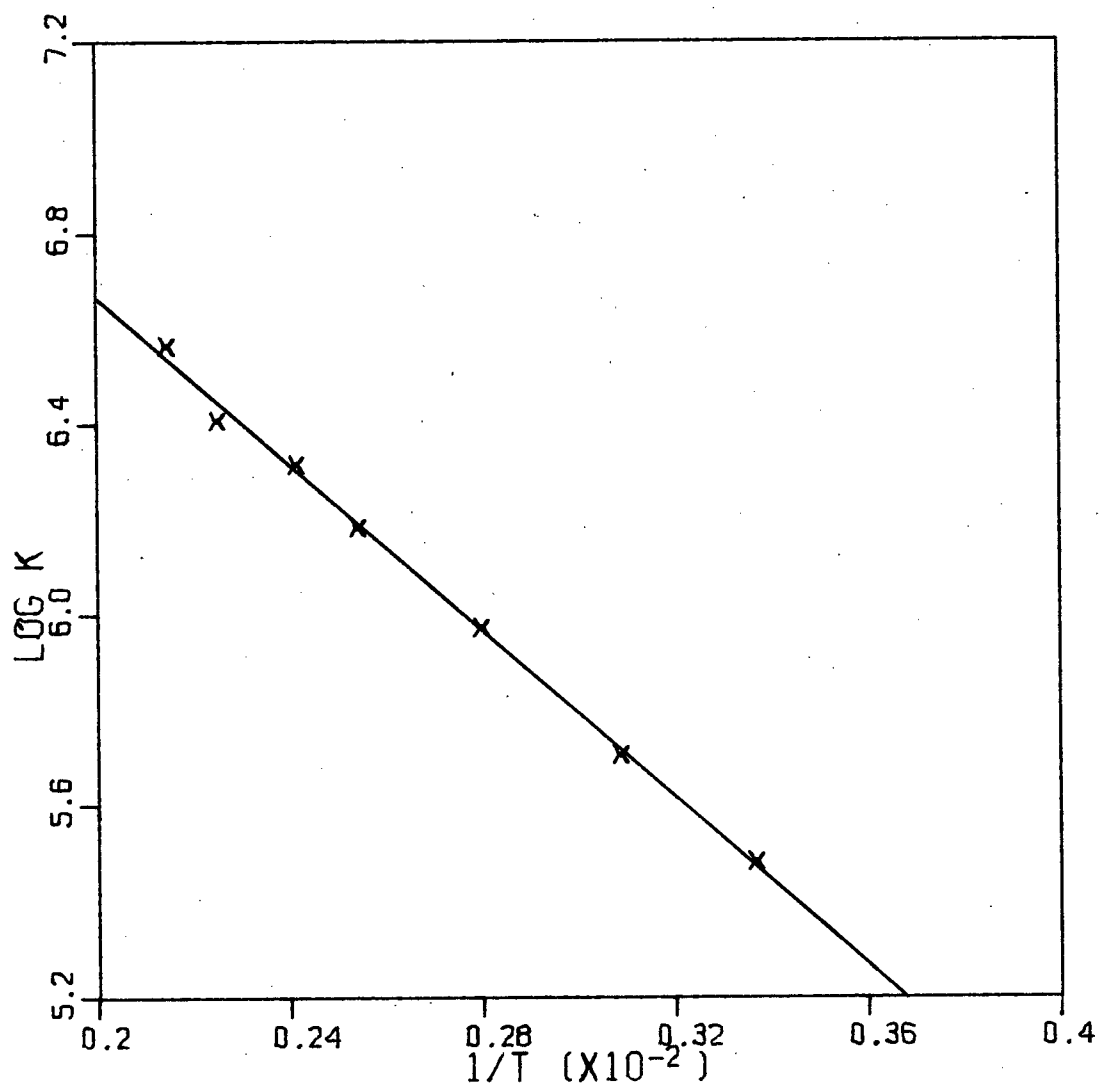
CIS BUTENE

Figure 11. Arrhenius plot?



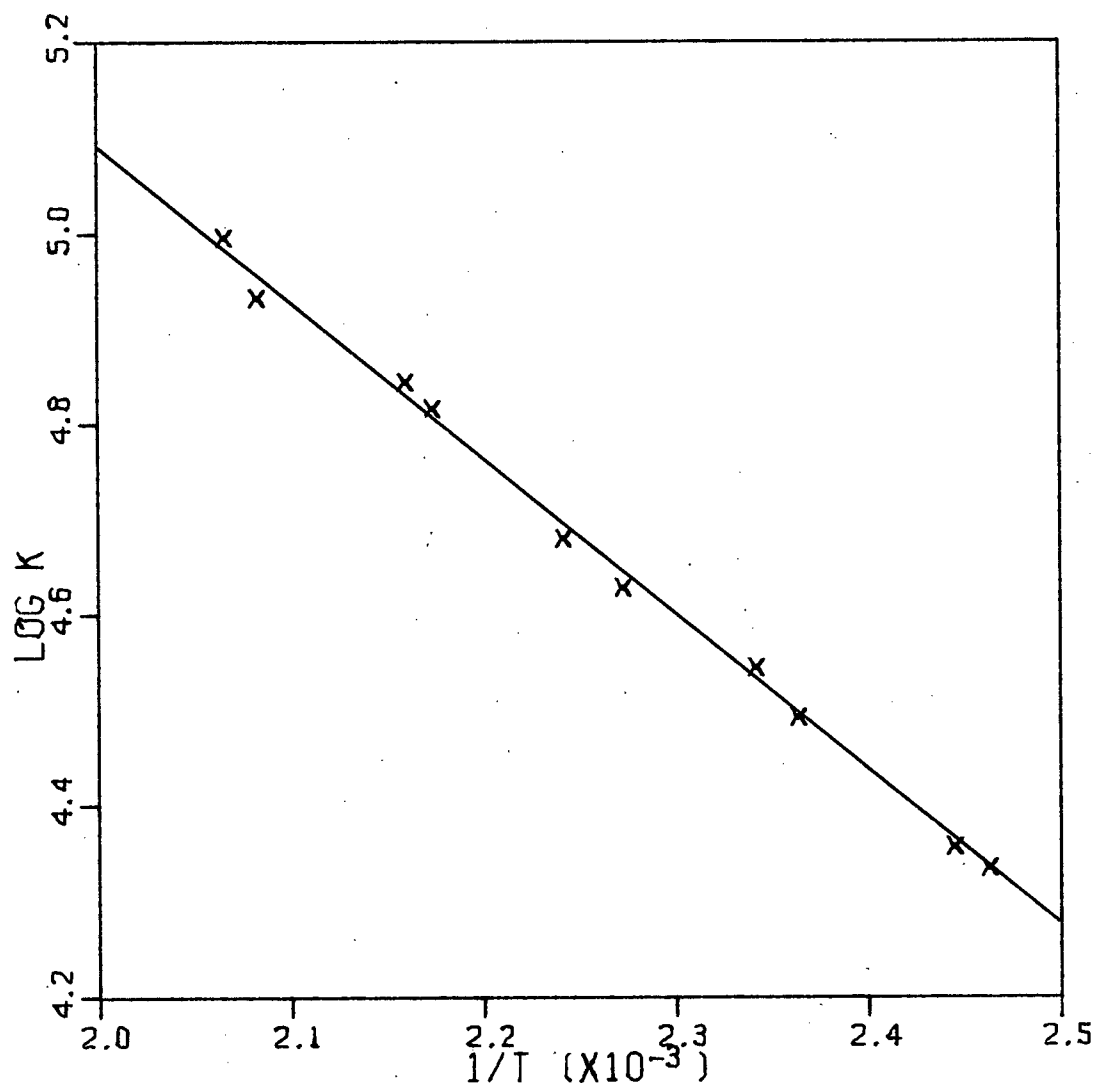
TRANS BUTENE

Figure 12. Arrhenius plot:



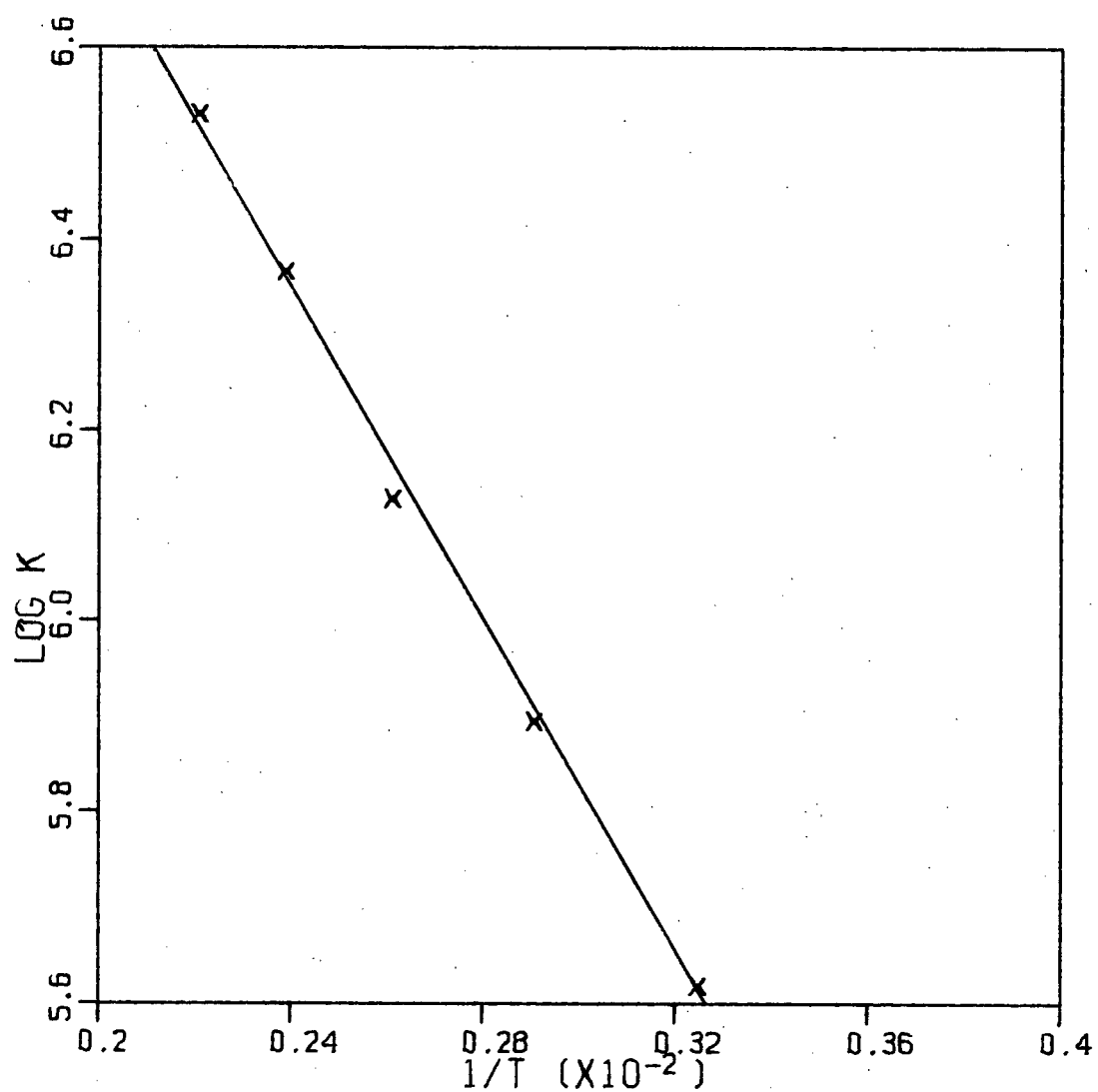
## DIMETHYL CYCLOHEXENE

Figure 13. Arrhenius plot



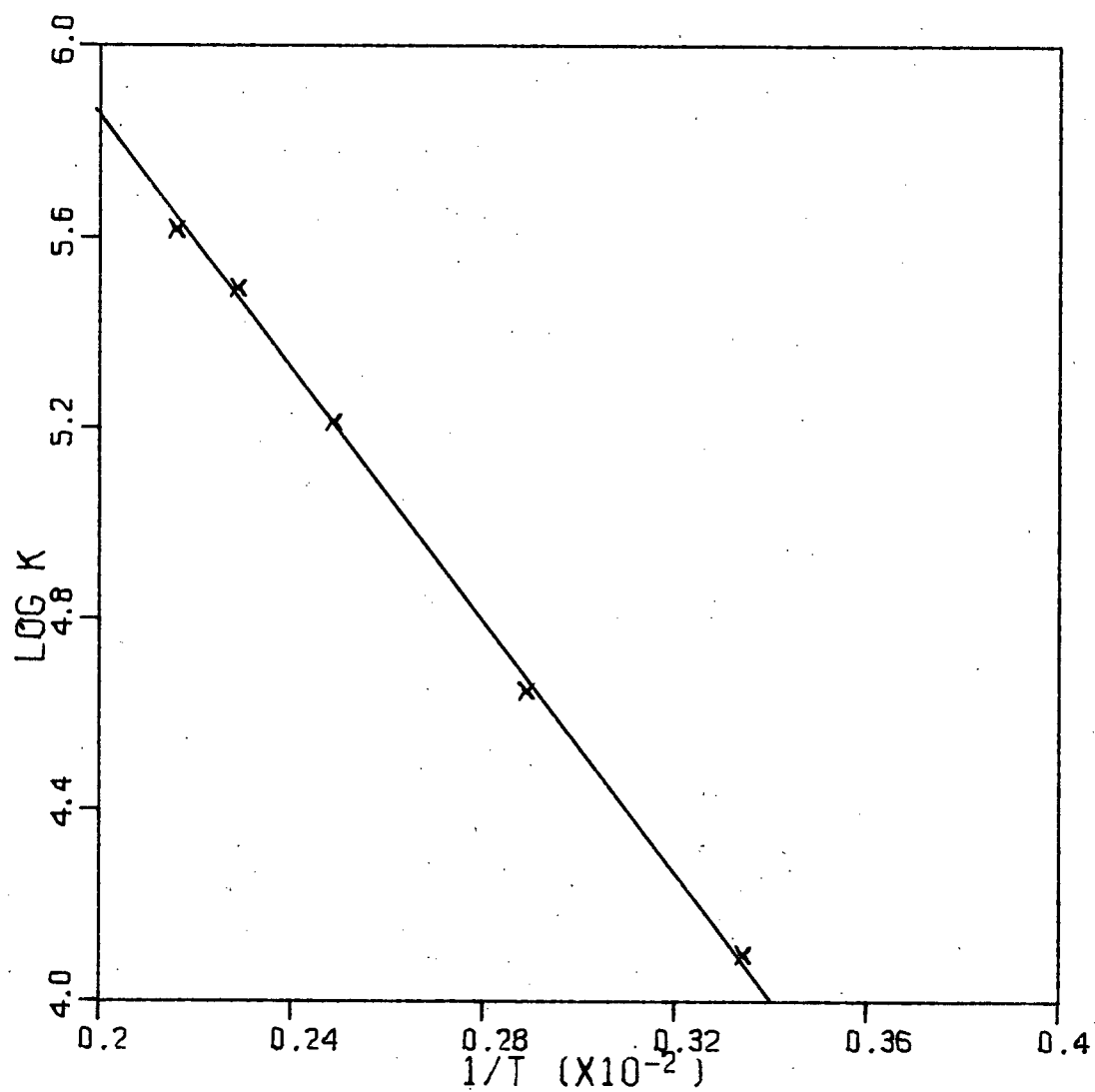
## METHYL CYCLOHEXENE

Figure 14. Arrhenius plot



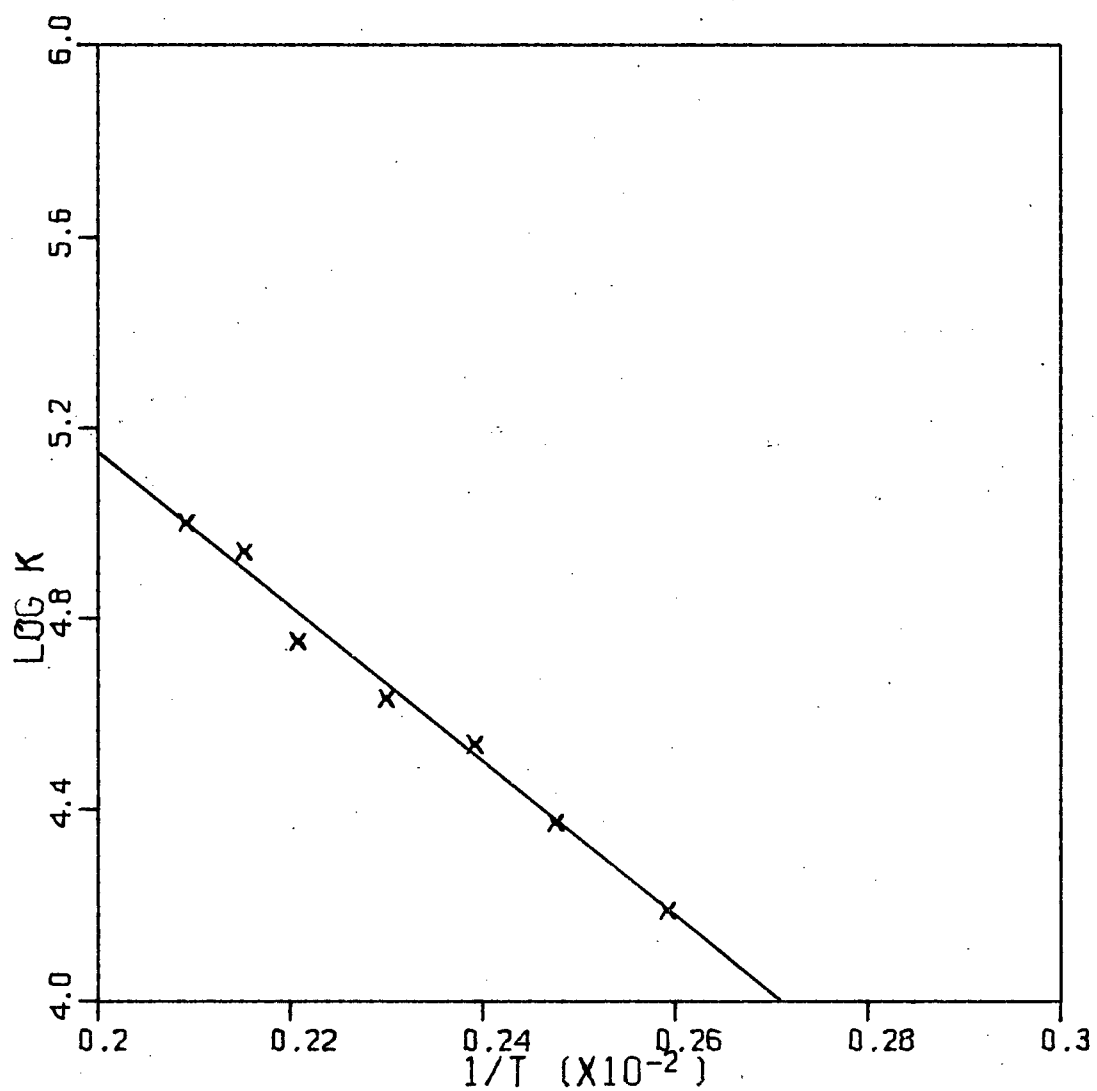
## DIMETHYL CYCLOPENTENE

Figure 15. Arrhenius plot.



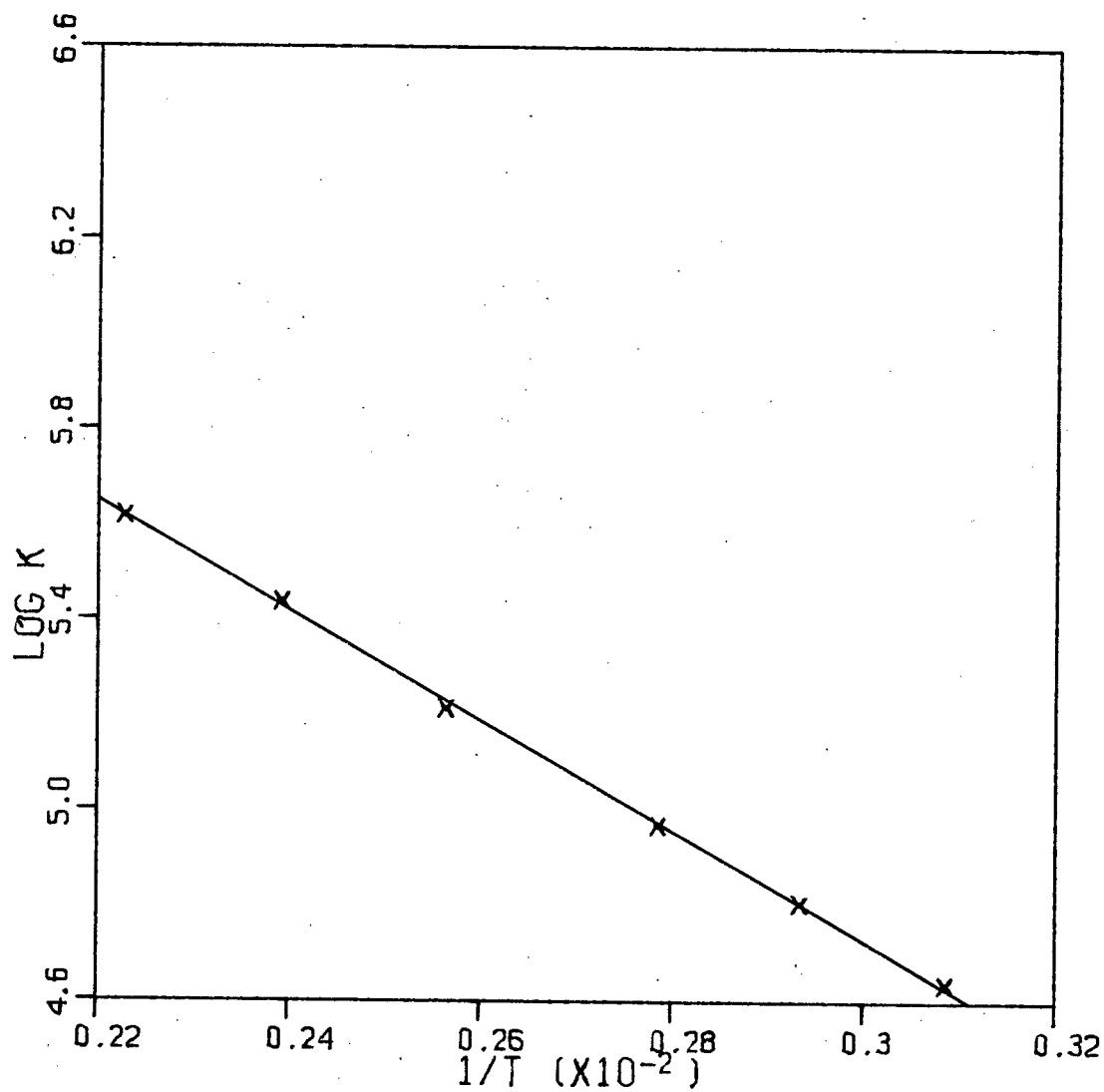
# METHYL CYCLOPENTENE

Figure 16. Arrhenius plot



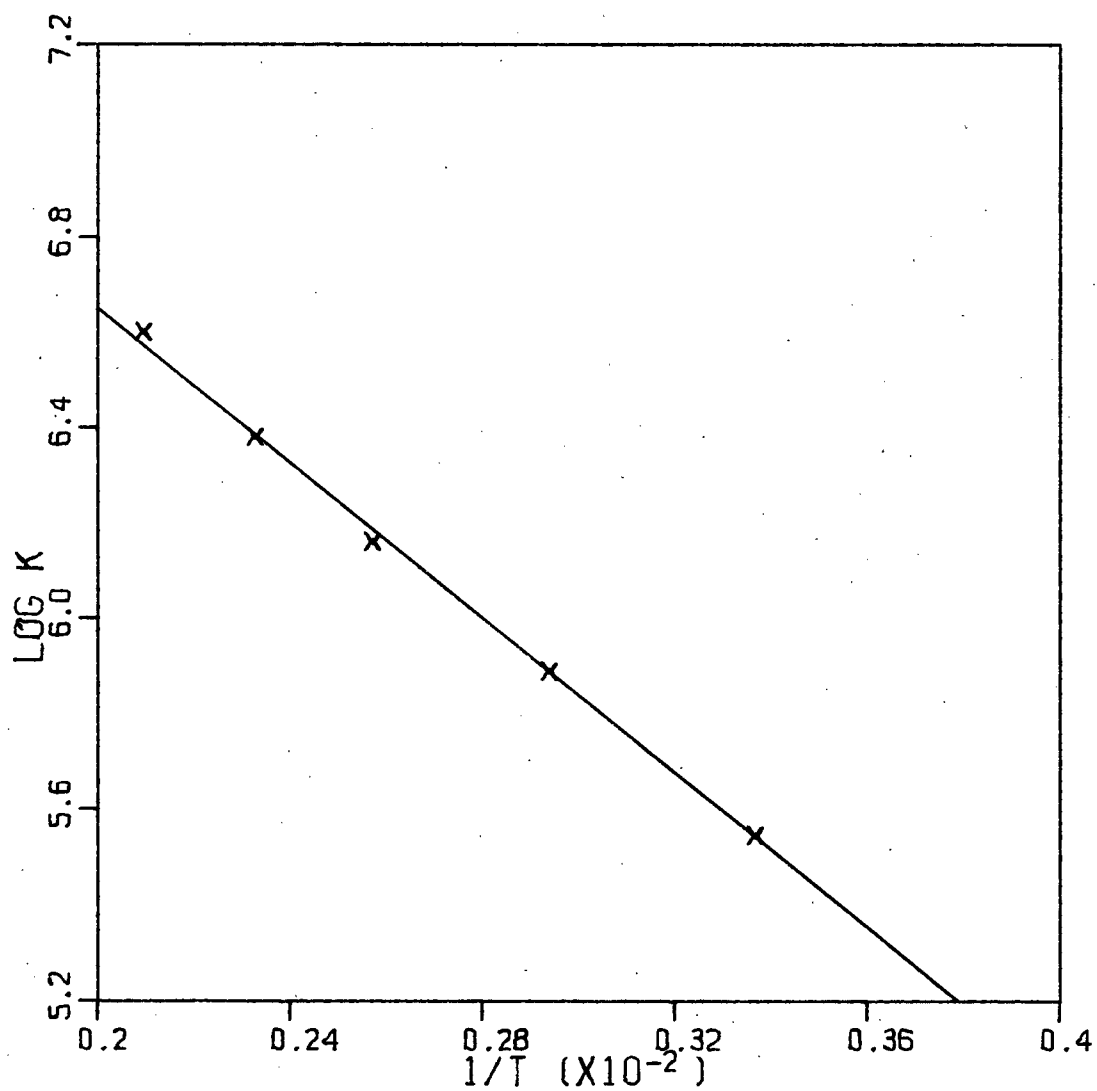
## CYCLOPENTENE

Figure 17. Arrhenius plots.



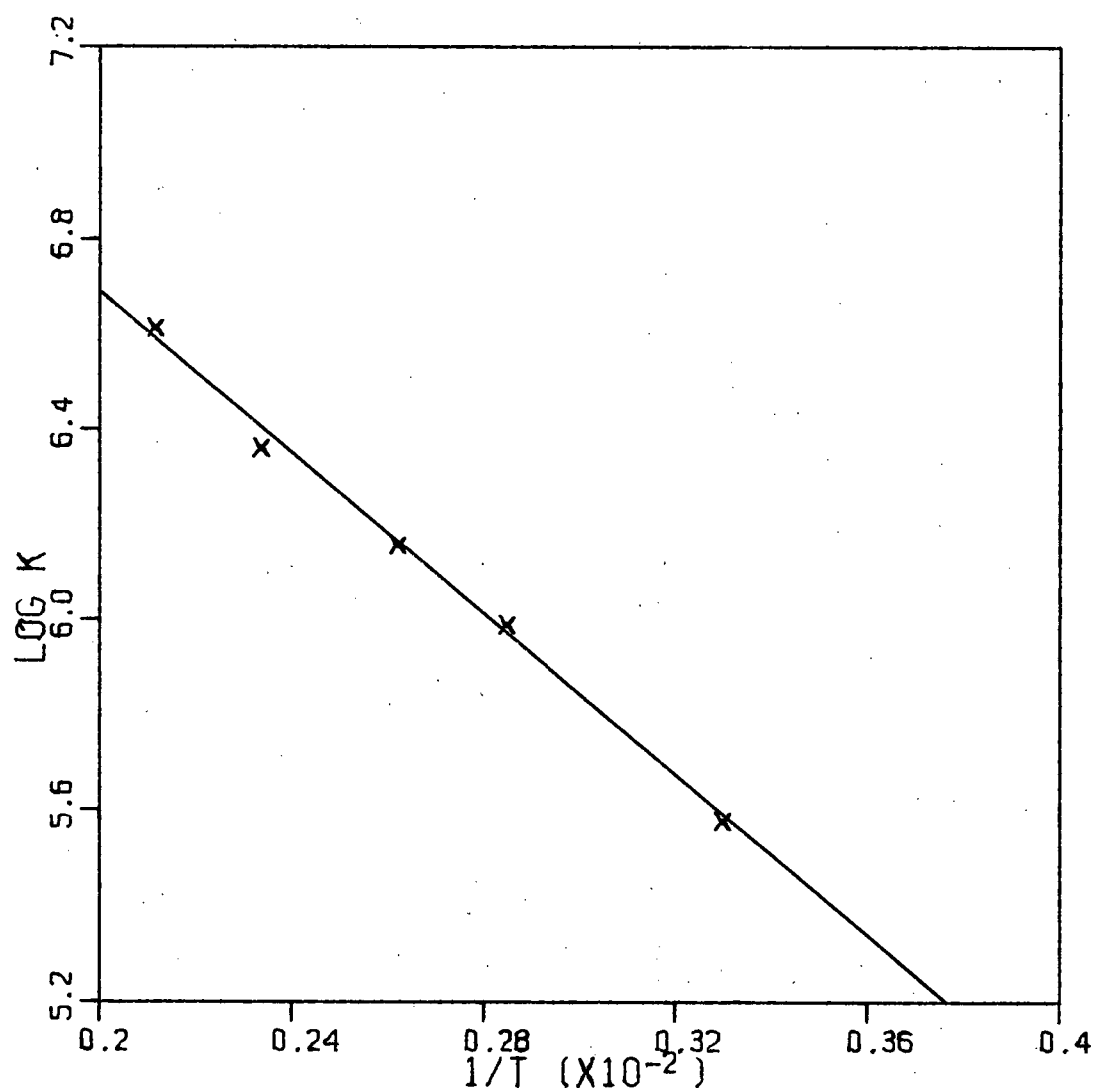
FURAN

Figure 18. Arrhenius plot



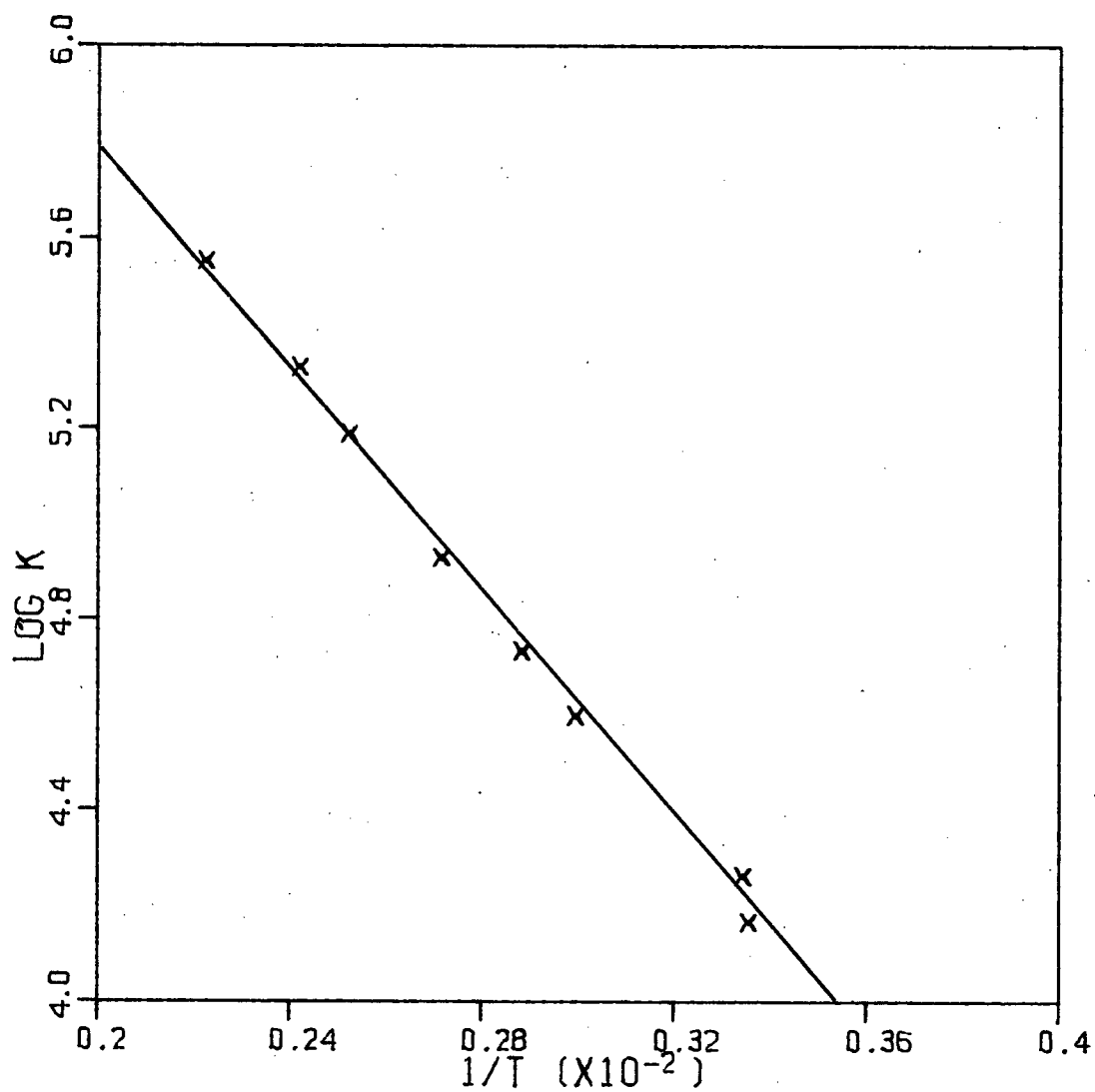
# METHYL FURAN

Figure 19. Arrhenius plot:



## CYCLOPENTADIENE

Figure 20. Arrhenius plot.



# CYCLOHEXADIENE

Figure 21. Arrhenius plot

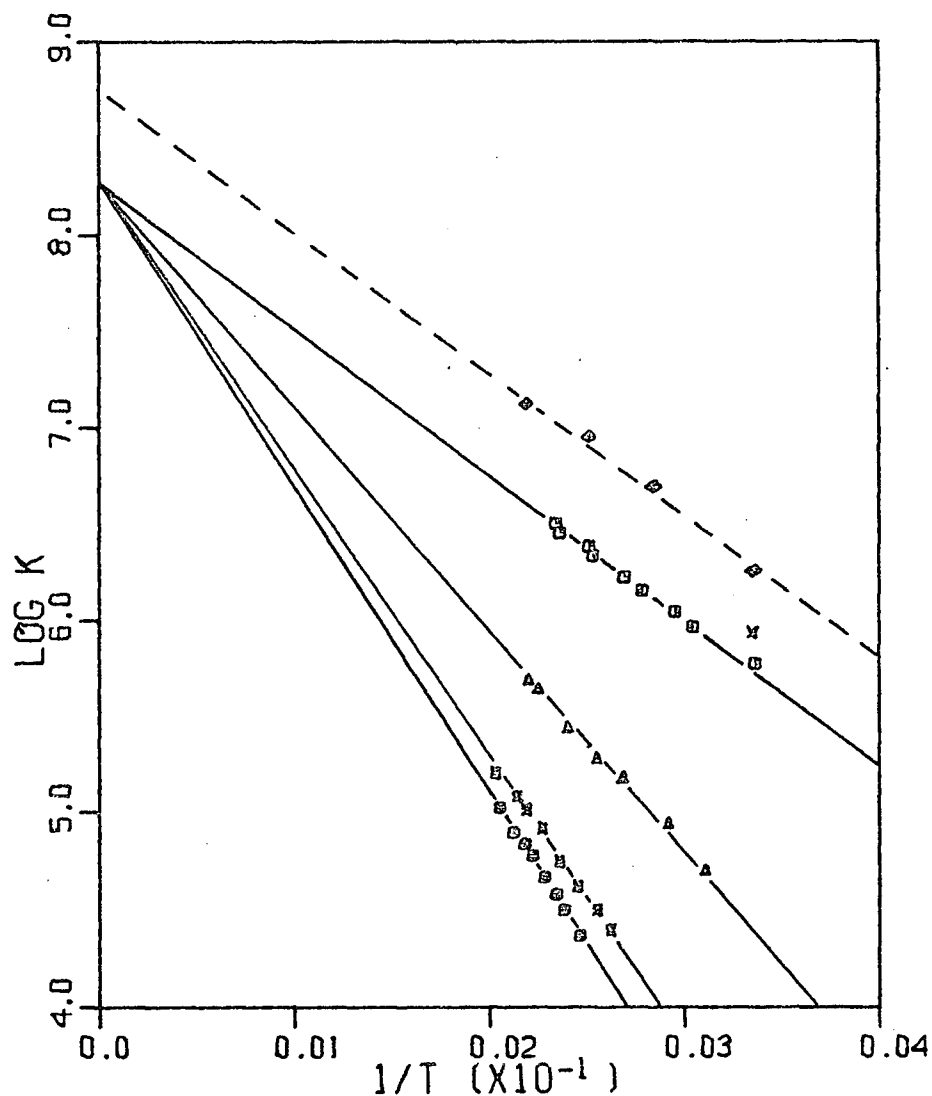
the  $O_2(^1\Delta_g)$  concentration as well as  $H$  and  $H_o$  at each temperature.  $K_r$  was obtained by direct substitution of these values into Equation (35), after making due allowance for the increase in flowrate and  $6340 \text{ \AA}$  emission with temperature, which is necessary because of the collision-induced nature of this band. Fortunately this effect has been well studied by Arnold, Browne and Ogryzlo (60) who found it to be small in magnitude, requiring a change of only  $\sim 0.60$  Kcals/mole in the final computation of the activation energy.

The preexponential A factors and activation energies for each compound were obtained from the intercept and slope of the  $\log(k_r)$  vs.  $1/T$  plots shown in Figs. 9 to 21, respectively. Activation energies obtained by a least squares analysis of these points are listed in Table 18, together with the rate constants extrapolated to room temperature. The errors that are quoted are the 95% confidence limits of the point distribution; they tend to be somewhat greater for the slower members of the series because of the narrower temperature range that was used for these compounds. The errors on the A factors are not independent of those on the activation energies but are related through the slope and mean point of the graph. The upper limit to the rate constant for cyclohexene was established by assuming that a change in the peak height of  $\sim 2\%$  would be observable, thus setting the  $\ln(H_o/H)$  value to 0.0198. A clearer idea of the relative values of these results can be obtained by looking at Figs. 22 to 25 in which the plots of Figs. 9 to 21 are displayed on a smaller scale along with the data of Hollingen and Timmons (55) and Herron and Huie (54), included for comparison purposes. The disagreement in these two sets of data for

Table 18. The preexponential factors and activation energies for the  $O_2(^1\Delta_g)$ -olefin reaction.

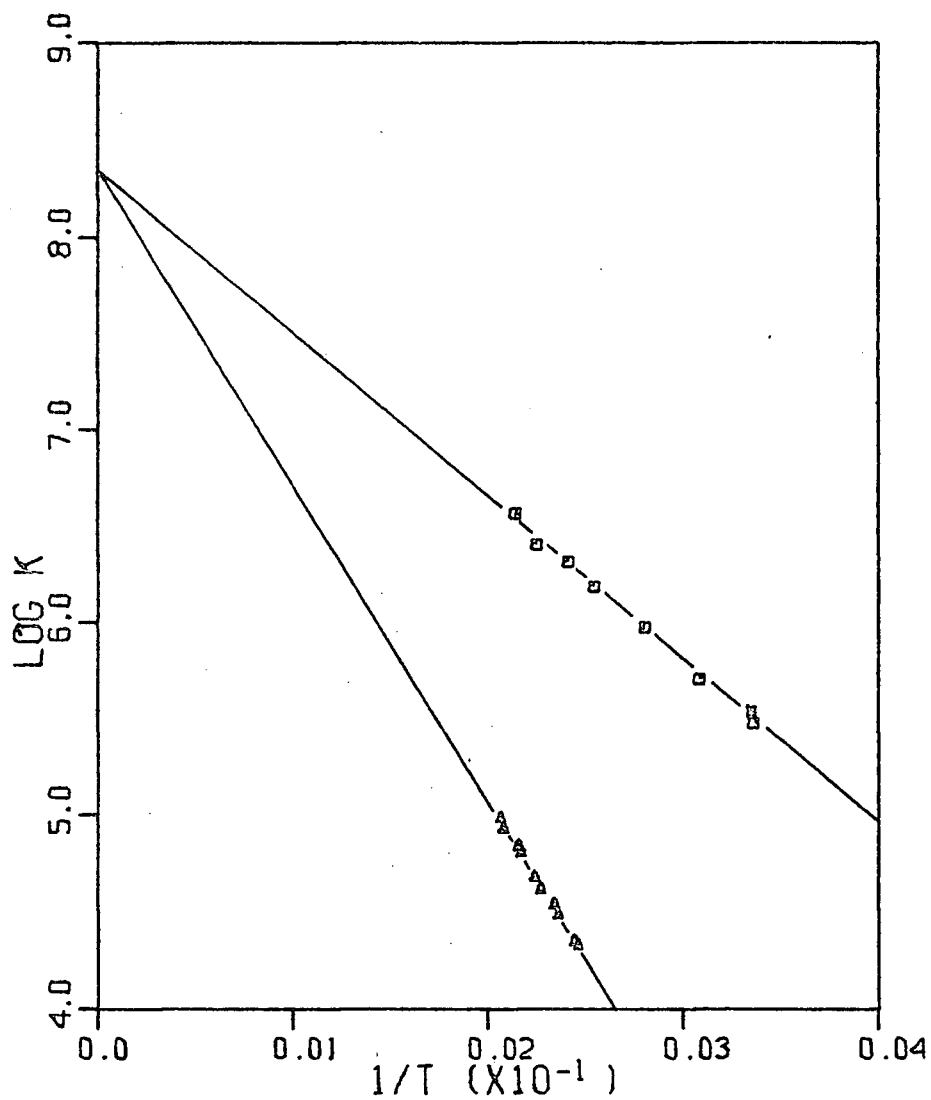
Compound	$\log_{10} (A)$ (litres/mole sec)	Activation energy kcal/mole	Room Temperature Rate constants (litres/mole sec)
2,3-dimethyl butene-2	$8.13 \pm 0.09$	$3.23 \pm 0.15^*$	$5.87 \times 10^5$
2-methyl butene-2	$8.02 \pm 0.16$	$4.86 \pm 0.28$	$2.88 \times 10^4$
cis-butene-2	$8.10 \pm 0.14$	$6.47 \pm 0.28$	$2.30 \times 10^3$
trans-butene-2	$8.30 \pm 0.18$	$7.29 \pm 0.36$	$9.05 \times 10^2$
1,2-dimethyl cyclohexene	$8.41 \pm 0.11$	$3.99 \pm 0.18$	$3.03 \times 10^5$
1-methyl cyclohexene	$8.38 \pm 0.15$	$7.52 \pm 0.30$	$7.31 \times 10^2$
cyclohexene	8.40 (assumed)	$>8.2^\dagger$	$<5 \times 10^2$
1,2-dimethyl cyclopentene	$8.46 \pm 0.16$	$4.02 \pm 0.28$	$3.21 \times 10^5$
1-methyl cyclopentene	$8.46 \pm 0.16$	$5.98 \pm 0.28$	$1.18 \times 10^4$
cyclopentene	$8.37 \pm 0.36$	$7.39 \pm 0.71$	$8.95 \times 10^2$
furan	$8.17 \pm 0.10$	$5.25 \pm 0.17$	$2.09 \times 10^4$
2-methyl furan	$8.30 \pm 0.12$	$3.76 \pm 0.22$	$3.50 \times 10^5$
1,3-cyclopentadiene	$8.38 \pm 0.19$	$3.89 \pm 0.32$	$3.42 \times 10^5$
1,3-cyclohexadiene	$8.20 \pm 0.16$	$5.47 \pm 0.26$	$1.55 \times 10^4$

$^\dagger$  Calculated from an upper limit of  $4 \times 10^4$  at  $200^\circ\text{C}$ ;  $^*$  Errors calculated using the algorithm given in Ref. 61 - 95% confidence limits quoted.



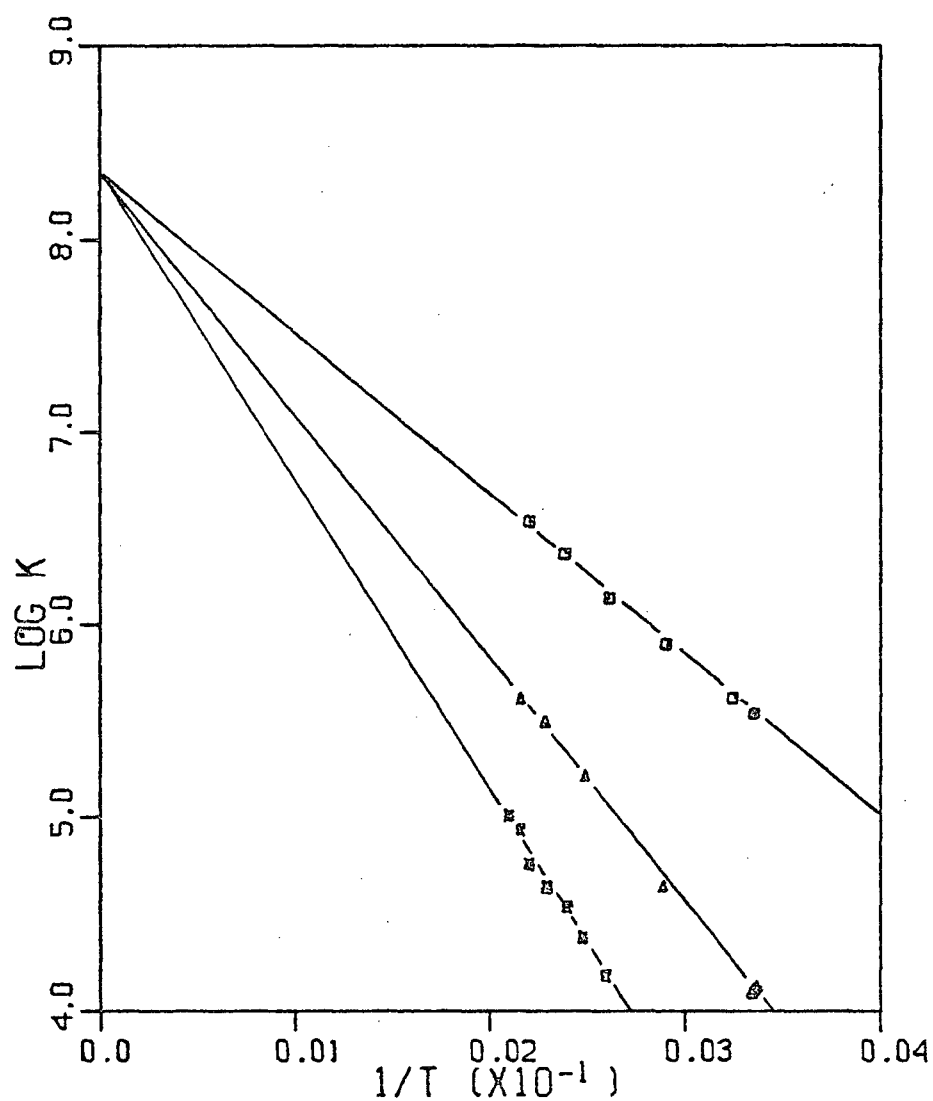
- = 2.3 DIMETHYL BUTENE-2
- Δ = 2 METHYL BUTENE-2
- x = CIS BUTENE-2
- = TRANS BUTENE-2
- ◆ = 2.3 DIMETHYL BUTENE-2 (REF:55)
- x = 2.3 DIMETHYL BUTENE-2 (REF:54)

Figure 22. Arrhenius plot.



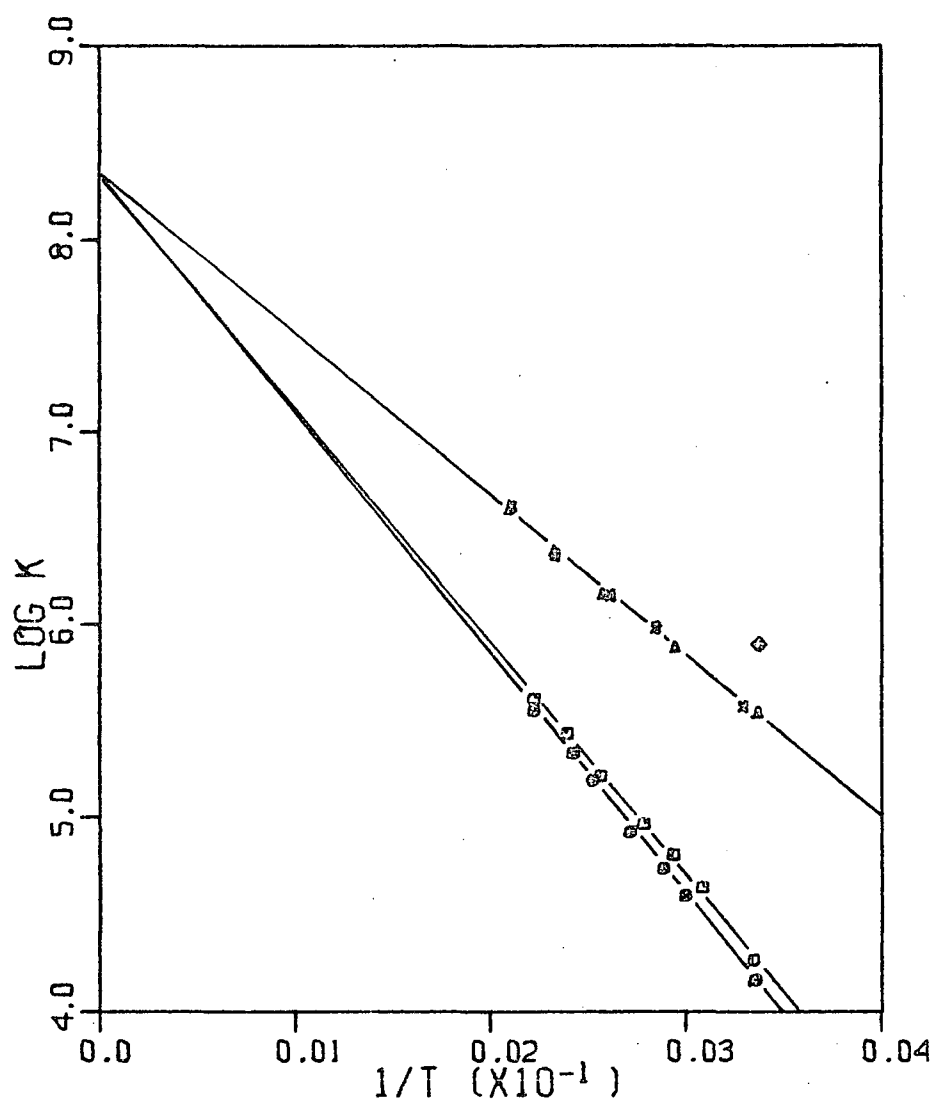
- = DIMETHYL CYCLOHEXENE
- △ = METHYL CYCLOHEXENE
- ⊠ = DIMETHYL CYCLOHEXENE (REF:54)

Figure 23. Arrhenius plot.



- = DIMETHYL CYCLOPENTENE
- △ = METHYL CYCLOPENTENE
- = CYCLOPENTENE
- ◻ = DIMETHYL CYCLOPENTENE (REF:54)
- ◊ = METHYL CYCLOPENTENE (REF:54)

Figure 24. Arrhenius plot.



- = FURAN
- △ = METHYL FURAN
- \* = CYCLOPENTADIENE
- = CYCLOHEXADIENE
- ◇ = CYCLOHEXADIENE (REF:54)

Figure 25. Arrhenius plot.

2,3-dimethylbutene-2 is somewhat disheartening, but can probably be attributed to the presence of a small quantity of atomic oxygen in the flow system of Hollinden and Timmons, for, even though they checked for the presence of an atomic oxygen absorption signal with their ESR spectrometer, it seems doubtful that they could observe an atomic oxygen concentration of much less than 0.1% of the quencher concentration.\* Since the atomic oxygen reacts rapidly by a chain mechanism, rather higher rate constants might be expected. It is interesting to note, that compared with the room temperature values of Herron and Huie, the relatively much more rapid reaction with 2,5-dimethylfuran shows little disagreement as might be expected from a process fast enough to compete with the atomic oxygen radical reactions.

#### The Pressure Dependence of the $O_2(^1\Delta_g)$ -2,3-Dimethylbutene-2 Reaction

The effect of pressure on the  $O_2(^1\Delta_g)$ -2,3-dimethylbutene-2 was determined here at two pressures (3.0 torr and 1.0 torr) chosen to provide a direct comparison with the data of Ackerman, Pitts and Steer (56). The 2,3-dimethylbutene-2 was added through a fixed inlet situated a distance of 85 cm from the mass spectrometer sampling leak and was observed using the parent peak at  $m/e = 84$ . The observed peak heights were used directly in equation (35) and the rate constants calculated at these two pressures. The results are shown in Table 19. It can be seen that, within the scatter of the points, no pressure dependence of

---

\* This assumes a  $10^{12}$  absolute spin sensitivity for detection of the  $O(^3P)$  by the ESR spectrometer (62) and a  $2\text{ cm}^3$  cavity in conjunction with the pressures and flowrates given by Hollinden and Timmons.

Table 19. Rate constants for the  $O_2(^1\Delta_g)$ -2,3-dimethyl butene-2 reaction at different pressures.

Pressure (torr)	Flowrate (cm/sec)	H/H <sub>o</sub>	$^1\Delta_g$ concentration (moles/litre)	Rate constant (litre mole <sup>-1</sup> sec <sup>-1</sup> )
0.98	63.30	0.200	$2.03 \times 10^{-6}$	$6.0 \times 10^5$
0.99	65.41	0.299	$1.64 \times 10^{-6}$	$5.7 \times 10^5$
1.03	63.31	0.251	$1.84 \times 10^{-6}$	$5.6 \times 10^5$
2.37	67.60	0.479	$1.09 \times 10^{-6}$	$5.9 \times 10^5$
2.40	68.99	0.484	$9.84 \times 10^{-6}$	$6.0 \times 10^5$

the rate constant is apparent.

These results are in direct conflict with the results and mechanism published by Ackerman, Pitts and Steer (56), but are in accordance with the similar findings of Furukawa and Ogryzlo (51) as well as Herron and Huie (53). Since no mention of the identity of the proposed intermediate in this reaction was made by Ackerman, Pitts and Steer, any direct criticism of their reaction is difficult. Their mechanism, however, requires the intervention of a long-lived intermediate in the reaction mechanism, a conclusion which is contrary to findings of the solution studies on this reaction. The possibility that the apparent rate increase at low pressure is due to the presence of atomic oxygen in their flow tube is strongly suggested by the fact that their result was not reproducible in the present system, in which all traces of atoms were removed by the addition of a small quantity of  $\text{NO}_2$  to the singlet oxygen flow.\*

---

\*

In a very recent paper, Herron and Huie indicate that this reaction is considerably more complicated than at first thought. No definite conclusions, however, were drawn for their data (73).

## DISCUSSION

### Comparison with $O_2(^1\Delta_g)$ Decay Studies

With the results of the present work, it is now possible to make a preliminary comparison between the directly determined  $k_r$  values of Table 18 and the  $(k_r + k_q)$  rate constants obtained from the increased  $O_2(^1\Delta_g)$  decay with added olefin. This is given in Table 20 for the two  $(k_r + k_q)$  determinations that have been made so far, together with the reactivities of the individual olefins in solution.

The large disparity in the two values of  $(k_r + k_q)$  necessitates that a choice is made between these two sets of data which, in the absence of any separate empirical evidence, can only be based on the fact that the difference probably results from the presence of atoms in the flow tube, an impurity which has commonly been found to produce an increase in the observed reaction rate of a particular olefin. Thus, the somewhat lower values of Ackerman, Pitts and Steer might be expected to be the more reliable of the two determinations. This conclusion would also be indicated by the reasonably good agreement between the  $(k_r + k_q)$  and  $k_r$  values of 2,3-dimethylbutene-2, 2-methyl butene-2 and trans butene-2, provided one ignores the anomalous position of cis butene-2 in this sequence, which cannot be attributed to a high  $k_r$  or  $k_q$  value that would fit in with the rest of the data on this series. A redetermination of this point in the guaranteed absence of atomic oxygen

Table 20. A comparison of the rate constants for reaction ( $k_r$ ) and quenching ( $k_q$ ) in the  $O_2(^1\Delta_g)$ -olefin system at 25°C.

Compound	$(k_r + k_q)$ (litres mole <sup>-1</sup> sec <sup>-1</sup> )		$k_r$ (litres mole <sup>-1</sup> sec <sup>-1</sup> )	$k_r$ (relative) in solution
2,3-dimethyl butene-2	7.5 x 10 <sup>5</sup> *	4.6 x 10 <sup>5</sup>	5.87 x 10 <sup>5</sup>	1.0
2-methyl butene-2	1.0 x 10 <sup>5</sup>	1.4 x 10 <sup>4</sup>	2.88 x 10 <sup>4</sup>	0.055
cis-butene-2	2.5 x 10 <sup>4</sup>	1.3 x 10 <sup>4</sup>	2.30 x 10 <sup>3</sup>	-
trans-butene-2	1.0 x 10 <sup>4</sup>	3.0 x 10 <sup>3</sup>	9.05 x 10 <sup>2</sup>	-
1,2-dimethylcyclohexene	-	-	3.03 x 10 <sup>5</sup>	0.10
1-methylcyclohexene	1.0 x 10 <sup>4</sup>	-	7.31 x 10 <sup>2</sup>	0.0025
cyclohexene	-	-	-	0.00012
1,2-dimethyl cyclopentene	-	-	3.21 x 10 <sup>5</sup>	-
1-methyl cyclopentene	4.0 x 10 <sup>5</sup>	-	1.18 x 10 <sup>4</sup>	0.045
cyclopentene	-	-	8.95 x 10 <sup>2</sup>	0.0029
1-methylfuran	-	-	3.50 x 10 <sup>5</sup>	-
furan	-	-	2.09 x 10 <sup>4</sup>	-
cyclopentadiene	8.8 x 10 <sup>6</sup>	-	3.42 x 10 <sup>5</sup>	-
1,3-cyclohexadiene	2.3 x 10 <sup>5</sup>	-	1.58 x 10 <sup>4</sup>	-
References	(50)	(52,56)	present work	(14)

\* Ref. 51 - obtained with NO<sub>2</sub> added (9.5 x 10<sup>5</sup> obtained previously in absence of NO<sub>2</sub>).

would certainly be helpful in clarifying this situation.

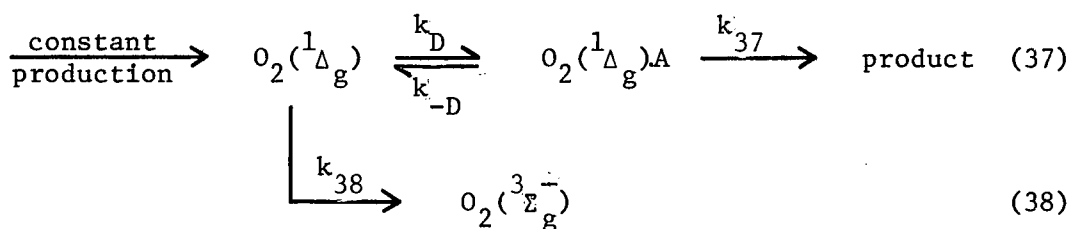
Assuming that this interpretation of the data is correct then, one can conclude that for these compounds,  $k_r \gg k_q$ , with a significant contribution to the  $(k_r + k_q)$  value for trans butene-2 coming from the quenching process. The slight discrepancy that remains between these two sets of data is probably the result of experimental error in the determination of the  $(k_r + k_q)$  or  $k_r$  rate constants, although the good agreement between the present work and the reevaluated rate constants of Herron and Huie (57) as well as Furukawa and Ogryzlo (51) would certainly not indicate that it is the  $k_r$  determination that is at fault in this respect.

Thus it is suggested that the quenching rate constants for these olefins would not be expected to differ substantially from those of the alkanes or lower alkenes and could probably be obtained to a fair approximation by simple extrapolation through the particular homologous series (52). Certainly by comparison with the amines, which are known to be considerably more efficient than the olefins in forming charge-transfer complexes and consequently at quenching  $O_2(^1\Delta_g)$ , these compounds would be regarded as being rather inefficient in their quenching ability.

#### Comparison with Other Temperature Dependence Studies

Apart from the data of Hollinden and Timmons, only one other temperature dependence study has been undertaken for the  $O_2(^1\Delta_g)$ -olefin reaction. This was performed by Koch (63,64), who generated the  $O_2(^1\Delta_g)$  by energy transfer from a triplet sensitizer in methanol solution and determined the  $\beta$  values (ratio of rate of  $O_2(^1\Delta_g)$  deactivation to rate of product formation) for each of the reactions between 20°C and -120°C.

By careful analysis of the variation in these parameters with temperature using the following reaction scheme:-



he was able to separate out the contributions from diffusion and side-reaction to the overall reaction rate, and so obtain an estimate of the activation energy for the photooxidation reaction.\* Table 21 lists these activation energies for the compounds of interest here along with the approximate rate constants.

In spite of the rather erratic behaviour of the solution data, it is evident that the large disparity between these two determinations of the activation energy is a real effect and cannot simply be attributed to physical error on the points. The gross trends in the series are

\* Assuming a steady state  $[\text{O}_2(^1\Delta_g)A]$  concentration:-

$$\beta = \frac{k_{38} [^1\Delta_g]}{k_{37} [^1\Delta_g \cdot A]} = \frac{k_{38}}{k_{-D} \cdot k_D} (k_{-D} + k_{37}) \quad (39)$$

$$\text{which gives: } k_{37} = k_{38} k_{-D} / \beta k_D \quad (40)$$

where the process is diffusion controlled and:-

$$k_{38} = k_D \beta \quad (41)$$

where it is reaction controlled. Knowing the temperature dependence of  $k_D$  from previous work, they were able to calculate the activation energy for the rate of product formation ( $k_{37}$ ). They also estimated an absolute value for this quality using values for  $k_D$  and  $k_{-D}/k_D$  obtained in a previous publication.(65).

Table 21. A comparison of the solution and gas-phase temperature dependence data.

Compound	Methanol Solution <sup>†</sup>		Gas Phase	
	$k_r$ (room temp.) (sec <sup>-1</sup> )	Activation energy (kcal/mole)	$k_r$ (room temp.) (litres mole <sup>-1</sup> sec <sup>-1</sup> )	Activation energy (kcal/mole)
2,3-dimethyl butene-2	$2.1 \times 10^{10}$	0.5	$5.87 \times 10^5$	3.23
2-methyl butene-2	$2.3 \times 10^7$	1.6	$2.88 \times 10^4$	4.89
2-methyl pentene-2	$7.0 \times 10^6$	2.0	-	-
isobutylene	$9.0 \times 10^3$	5.7	-	-
butene-2	$1.1 \times 10^6$	10.0	$2.30/0.90 \times 10^3$	$6.47/7.29^*$
2-methylfuran	$6.2 \times 10^8$	0.4	$3.50 \times 10^5$	3.76
furan	$4.5 \times 10^8$	0.2	$2.09 \times 10^4$	5.25
cyclopentadiene	$3.6 \times 10^8$	0.3	$3.42 \times 10^5$	3.89
1,3-cyclohexadiene	$3.0 \times 10^7$	1.2	$1.58 \times 10^4$	5.47

<sup>†</sup> Rose Bengal sensitizer.

\* cis/trans

certainly the same in the two cases, with increasing methyl substitution or decreasing ring size producing a lowering in the activation energy.

This jump in the activation energies is somewhat surprising as there is little a priori reason for assuming any major difference (other than dielectric constant) between the reaction in solution and in the gas phase. A previous study by Foote and Denny (66,67) has shown that there is only a slight change in the  $\beta$  values or the product distribution for photooxidation of 2-methyl pentene-2 in different solvent mediums. They produced the singlet oxygen by energy transfer from a number of sensitizers dissolved in a series of solvents with dielectric constants ranging from 2.3 to 48.9. Even after compensating for the differing reaction rates, these  $\beta$  values changed by only a factor of four, indicating the involvement of a non-polar transition state that interacts with the surrounding medium to only a limited extent.

In normal Diels-Alder reactions it has generally been found that reaction in the gas-phase is similar to that in solution in that the preexponential A factors and the activation energies have approximately the same values in the two mediums (68,69). Unfortunately because it was necessary to separate the diffusion and reaction processes in his treatment of the data, the values quoted by Koch (63) for the A factors of the reaction refer to a unimolecular process and therefore cannot be compared directly with the bimolecular rate constants in the present work. The activation energies alone, however, suggest a difference in the reaction mechanism between the gas and solution phases.

This conclusion gains further support from a comparison of the product distributions in the gas (52) and solution phase (34,36), which

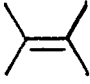
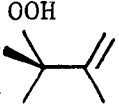


show that the products resulting from attack of the singlet oxygen at the two unsaturated carbon atoms of 2-methyl butene-2, for example, are much more evenly distributed between these two positions in the solution phase; in the gas phase, attack at the 2-position is about twice as efficient as that at position 3. This characteristic trend holds throughout the series of substituted olefins and contrasts quite strongly with the total absence of any solvent effect on the product ratio for 2-methyl pentene-2 (67). The reason for this discrepancy is unknown at present.

#### The Entropy of the Transition State

To gain some idea of the relationship between the structure of the transition state and that of the reactants and products, it is instructive to calculate the entropy change for the complete reaction and to compare it with the value of the entropy of activation  $\Delta S^\ddagger$  obtained here. Unfortunately, this can only be done in an approximate fashion as the  $\Delta S_0$  values for the products of these reactions have not yet been determined and must be estimated by the method of group additivity expounded by Benson (70). Such estimated values, however, are generally correct to within  $\sim 2.0$  e.u., which is sufficiently accurate for the present purposes. They are listed in Table 22 for 2,3-dimethyl butene-2 and cyclopentadiene. These compounds are taken as being representative of each series as little divergence would be expected between molecules that differ only in the structure of the substituent groups.

The value of the entropy of activation  $\Delta S^\ddagger$  can be obtained using the following equation:-

Table 22. The enthalpy and entropy changes in the reaction of  $O_2(^1\Delta_g)$  with 2,3-dimethyl butene-2 and cyclopentadiene

Compound	$\Delta H_f^\circ$ (kcal/mole)	$S_o$ (cals/deg mole)	$\Delta S_o$ (cals/deg mole)
	-15.91 <sup>c</sup>	86.67 <sup>c</sup>	-26
	-51 <sup>a</sup>	110 <sup>a</sup>	
O=O	23	49 <sup>b</sup>	
	32.4 <sup>c</sup>	~60 <sup>a</sup>	~30
	-20 <sup>a</sup>	~78 <sup>a</sup>	

<sup>a</sup> Estimated by group additivity methods (70).

<sup>b</sup> Assumed same as  $O_2(^3\Sigma_g^-)$

<sup>c</sup> From Ref. 71.

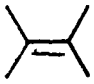
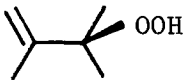
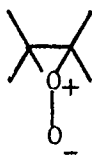

$$A = \frac{KT}{h} e^{\Delta S^\ddagger / R} \quad (42)$$

which is derived from a comparison of the Arrhenius and thermodynamic formulations of the reaction rate (72). By selecting a mean  $\log(A)$  value of 8.3 from the data shown in Table 18 and substituting it directly into equation (42), the  $\Delta S^\ddagger$  value is determined to be -22.4 e.u. Since  $A$  is expressed in litres mole<sup>-1</sup> sec<sup>-1</sup>, this is referred to a standard entropy state of unit molar concentration commonly used in such studies.

The apparent similarity in  $\Delta S^\ddagger$  and the change in the entropy for the reaction has often been taken to indicate that the transition state is similar in structure to the final product (69,72). An inspection of Table 22 will show that this deduction is applicable to the cyclopentadiene data; the difference in these two values probably reflects the greater rigidity of the final product.

The hydroperoxide reaction requires a little more careful consideration as several different pathways have been proposed for this reaction. In Table 23, the estimated standard entropies for the formation of the perepoxide and dioxetane transition states have been calculated. It can be seen that formation of both of these intermediates involves a large negative  $\Delta S^\ddagger$ , which would have to be reduced considerably by the formation of a much looser transition state in order to account for the observed results. The transition state for the proposed 'ene' mechanism cannot be calculated directly, but can be used to explain the  $\Delta S^\ddagger$  values obtained here by a weakening of the C-O bond (compared to the hydroperoxide product) that compensates for the decreased entropy of the cyclic transition state. The possibility that the transition state is

Table 23. The estimated entropy changes for the proposed intermediates in the  $O_2(^1\Delta_g)$ -2,3-dimethyl butene-2 reaction.

Structure	$S_o$ (cals/deg mole)	$\Delta S_o$ (cals deg <sup>-1</sup> mole <sup>-1</sup> )
$O=O$ 	135.67	-
	~110	-26
	~92 <sup>a</sup>	-43
	~87	-48

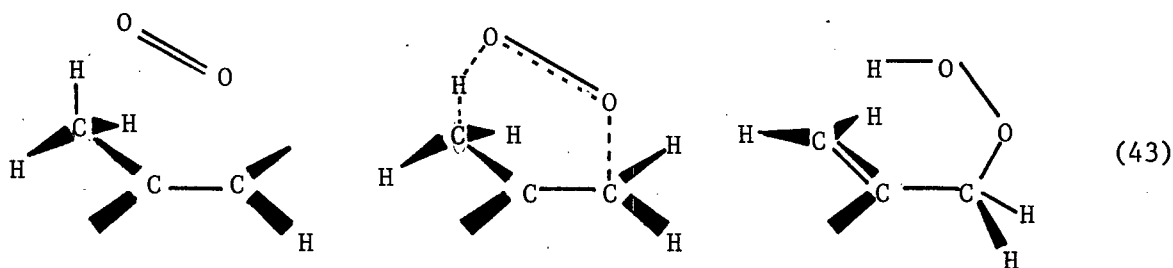
<sup>a</sup> Calculated by analogy with pentamethylcyclopropane (70).

like the final product is by no means as obvious in this case, even though there is a similarity in the magnitude of the entropy factors.

### The Transition State of the $O_2(^1\Delta_g)$ -Olefin Reaction

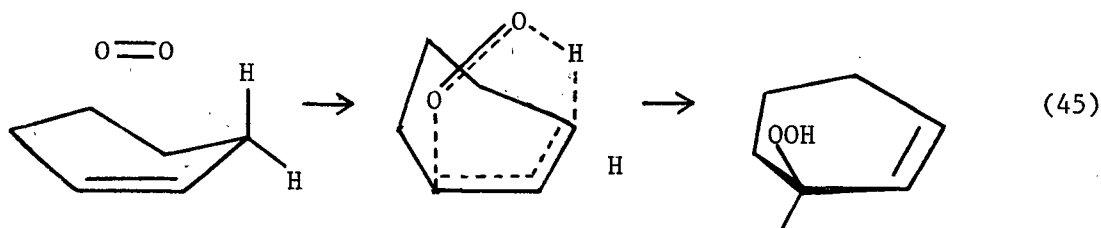
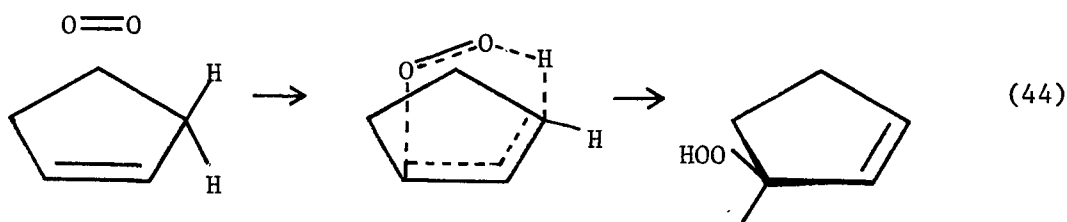
The most striking feature of the data shown in Table 18 is the rapid increase in the activation energies for the lower members of the cyclohexene series compared with the analogous compounds based on the cyclopentene structure. Because of the similarity in the substituents directly attached to the olefinic double bond, it seems likely that this effect cannot be attributed to a change in the electron density at the carbon atom, but is due to an increased energy requirement in the reaction of singlet oxygen with the six-membered ring compounds.

In the concerted addition to the olefin according to the 'ene' mechanism, the transition state geometry would be largely governed by the need to produce an adequate overlap of the p orbitals involving the 1,3 shift of the double bond. This would produce a near-planar  $sp^2$  arrangement of the three carbon atoms, with the singlet oxygen bonding from above or below the molecular plane:-



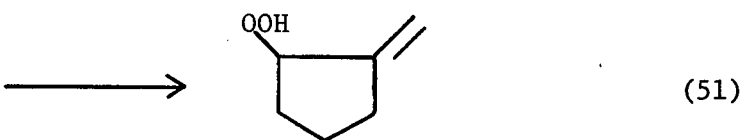
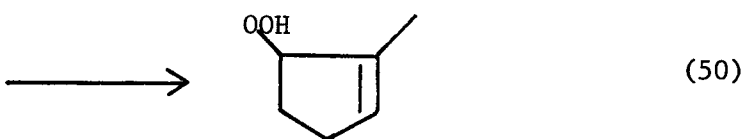
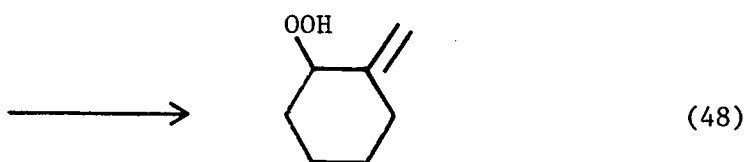
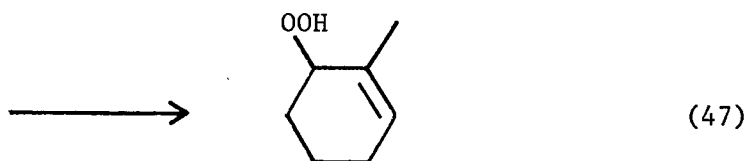
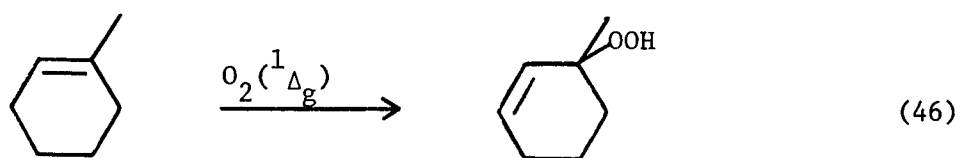
When applying this mechanism to the cyclopentene or cyclohexene compounds, an additional factor has to be taken into consideration as the conformation of the ring system now plays a major role in governing

the ability of a particular compound to produce the required transition state geometry. This results in the fact that, although the five-membered ring can maintain a near-planar configuration throughout the reaction, a six-membered ring compound is highly strained under such conditions and would probably prefer an arrangement in which the carbon atom opposite the double bond is bent out of the plane of the ring:-



The residual strain still associated with the six-membered ring compounds would show up as an increase in the activation energy for reaction of these compounds and is clearly illustrated by a comparison of the data on cyclohexene and cyclopentene (Table 18). Any distortion from this rigid planar arrangement of the olefin would result in a decrease in the strain energy of the cyclohexene compounds, but would also make the double bond shift a considerably more difficult process.

In the mono-methyl derivatives the situation is slightly more complicated as there are now several possible reaction pathways open to the olefin:-



A gas phase product distribution study has indicated that reaction is favoured by a greater degree of substitution at a particular carbon atom. This implies that reaction at the 1-position of each compound should have a substantially lower activation energy than reaction at the 2-position. Reaction (49) would thus be the preferred pathway for 1-methyl cyclopentene and reaction (46) for 1-methyl cyclohexene - although in this last case, a certain amount of competition from reaction (48) might be expected because of the higher activation energy for reaction within the ring. The net effect, however, would be an overall increase in the observed activation energy over the 1-methyl cyclopentene analogue.

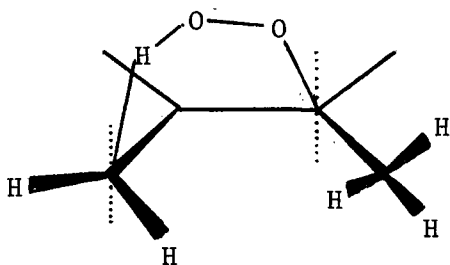
In dimethylcyclohexene, where reaction can occur in the side group, the activation energy would not be expected to be significantly higher than in dimethylcyclopentene.

One further indication of the geometry of the transition state is provided by a comparison of the activation energies for the cis and trans isomers of butene-2. Energetically these compounds are separated by a factor that results from the steric hindrance of the two methyl groups in cis butene-2, and shows up at a  $\sim 1.0 \text{ Kcal mole}^{-1}$  difference in the two heats of formation of these compounds. The observed change in the activation energies of  $0.7 \text{ kcal mole}^{-1}$  (or  $0.57 \text{ kcal mole}^{-1}$  if the A factors of the two compounds are made equal) must be produced by a reduction of this effect in the transition state, indicating an increased separation of the two sterically hindered methyl groups.

It is possible to make an approximate calculation of the distance between these two methyl groups by assuming that the steric hindrance decreases as the square of the distance between the closest approach of

the hydrogen atoms on each methyl group. Taking this distance to be  $1.56 \text{ \AA}$  in cis butene-2, and assuming that the trans isomer contributes nothing to the relative energy of the transition state, the separation of these two methyl groups can be estimated to be  $\sim 2.4 \text{ \AA}$  in the transition state, a distance which is considerably greater than that obtained using the planar olefin model suggested previously. This situation is not alleviated to any great extent by assuming a certain amount of  $sp^3$  character in the unsaturated carbon atoms.

Although this discrepancy can probably be attributed to the experimental error on the points, it is possible that it is a real effect resulting from a twisting of the transition state in order to produce a less strained singlet oxygen bridge between the 1 and 3 positions of the double bond. An increased separation of the sterically hindered methyl groups would then result from the rotation of these two groups:-



(52)

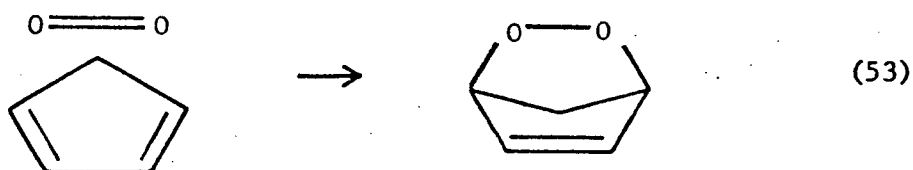
Whether or not this transition state would agree with the previous conclusions regarding the effect of the ring size on the reaction rate, would depend solely on the angle of twist and the amount of distortion of the olefin from the required planar arrangement. Any further speculation on this point, however, cannot be justified by the reliability

of the experimental results which should be interpreted as showing a small difference in the activation energies of the two isomers of butene-2, rather than the exact magnitude of this quantity.

It is difficult to provide an adequate explanation of these results using either of the alternative peroxide (equation (17)) or dioxetane (equation (19)) mechanisms. If it is the formation of the intermediate that defines the rate controlling step, then the reaction would be localized at the double bond and one would not expect the ring size to have any effect on the observed activation energy. This is obviously not the case. Conversely, if the slow process is that of the rearrangement of the intermediate to the product, there is difficulty in explaining the higher activation energy of methyl cyclohexene when, instead of reaction within the ring, the removal of hydrogen from the methyl group would provide the more favourable pathway, with an activation energy similar to that for methyl cyclopentene. Both of these objections provide major obstacles to any coherent explanation of the results in terms of these two mechanisms.

#### The Transition State of the $O_2(^1\Delta_g)$ -Diene Reaction

By comparison with the mono-olefins, the reaction of singlet oxygen with the dienes is a much simpler system for which there is little doubt as to the reaction mechanism. This has been found to follow a normal Diels-Alder process:-



An inspection of the data shown in Table 18 clearly illustrates the effect of the substituents at the 2- and 5-positions of the five-membered ring compounds in which the replacement of the hydrogen atom by the methyl group at the 2-position of the furan ring as well as the replacement of the oxygen by the  $\text{CH}_2$  group of the cyclopentadiene molecule causes a marked increase in the rate of reaction with singlet oxygen. In the first case, this effect is undoubtedly the result of the increased inductive effect of the methyl group producing a higher  $\pi$  electron density at the 2-position of the furan ring and so favouring attack by the electrophilic singlet oxygen; the latter case probably reflects the lower delocalization energy of the cyclopentadiene molecule.

Of rather more interest is the fact that the activation energy for the reaction of  $\text{O}_2(^1\Delta_g)$  with cyclohexadiene is some  $\sim 1.6$  Kcals mole<sup>-1</sup> higher than that with cyclopentadiene. This effect has also been noticed in the parallel reaction involving the Diels-Alder addition of maleic anhydride to these compounds, where it has been explained in terms of the greater separation of the 1- and 4-positions on cyclohexadiene. Since this distance is  $\sim 20\%$  greater than in cyclopentadiene (68) the maleic anhydride would have to stretch considerably further in order to produce the bicyclic transition state of the addition reaction, and might even produce a certain amount of distortion within the six-membered ring. As these difficulties would not be as great in cyclopentadiene, the somewhat lower activation energy observed experimentally (12.6 Kcals mole<sup>-1</sup> for cyclohexadiene; 8.8 Kcals mole<sup>-1</sup> for cyclopentadiene) would not seem at all unreasonable. Unfortunately on this model, the similarity in the bond lengths of the singlet oxygen and the maleic anhydride would require a similar difference in the activation energies

of these two compounds. Since this is obviously not the case it is evident that the reaction is more complicated than originally suggested, requiring a certain degree of involvement by the individual dieneophile. A much wider study would be needed, however, in order to provide a detailed explanation of this effect.

## CONCLUSIONS

The analysis of the results given here favours the 'ene' mechanism for the reaction of singlet oxygen with the mono-olefins. This is largely based on the fact that the observed change in the activation energies for the series of five and six membered ring compound can only be explained by the additional stereochemical requirements of a cyclic transition state similar to that predicted by such a mechanism. This effect cannot easily be explained by assuming either of the alternative mechanisms that have been proposed for this reaction.

It is thus suggested that the geometry of the transition state is probably governed by the 1,2-shift of the olefinic double bond, requiring a near-planar arrangement of the olefin molecule, with the singlet oxygen situated directly above or below this plane. A slight twisting of the transition state, suggested by the decrease in the steric hindrance in cis-butene-2, would also fit in well with the expected geometry under these conditions.

A comparison of the temperature dependence and product distribution studies on these reactions indicates that there is a considerable disparity between the solution and gas phase data, although each forms a more or less consistent set within itself.

Finally, a comparison of the rates of these reactions with the data obtained in  $O_2(^1\Delta_g)$  removal studies, suggests that the contribution from physical quenching in these systems is small with rate constants probably of a similar magnitude to the homologous alkane or alkene molecules.

REFERENCES

1. Gilmore, F.R., J.Q.S.R.T., 5, 369 (1965).
2. Ogryzlo, E.A., Photophysiology, 5, 35 (1970).
3. Griffith, J.S. Oxygen in Animal Organisms (Dickens, F. and Nieil, E., Eds.), 141 (1964) McMillan, N.Y.
4. Kearns, D.R., J. Amer. Chem. Soc., 91, 6554 (1969).
5. Herzberg, G. and Herzberg, L., Nature, 133, 759 (1934).
6. Van Vleck, J.H., Astrophys. J., 80, 161 (1934).
7. Ellis, J.W. and Kneser, H.O., Publ. Astron. Soc. Pac., 46, 106 (1934).
8. Ogryzlo, E.A., J. Chem. Educ., 42, 647 (1965).
9. Gray, E.W. and Ogryzlo, E.A., Chem. Phys. Letts., 3, 658 (1969).
10. Bader, L.W. and Ogryzlo, E.A., Disc. Far. Soc., 37, 46 (1964).
11. Derwent, R.G. and Thrush, B.A., Disc. Far. Soc., 2036 (1971).
12. Falick, A.M. and Mahan, B.H., J. Chem. Phys., 47, 4778 (1967).
13. Kautsky, H., Trans. Far. Soc., 35, 216 (1939).
14. Gollnick, K., Adv. Photochem., 6, 1 (1968).
15. Kearns, D.R., Chem. Revs., 71, 395 (1971).
16. Foote, C.S. and Wexler, S., J. Amer. Chem. Soc., 86, 3879 (1964).
17. Kawaoka, K. Khan, A.N. and Kearns, D.R., J. Chem. Phys., 46, 1842 (1967).
18. Browne, R.J. and Ogryzlo, E.A., Proc. Chem. Soc. (London), 117 (1964).
19. Murray, R.W. and Kaplan, M.L., J. Amer. Chem. Soc., 90, 537 (1968).
20. Wasserman, H.H. and Scheffer, J.R., J. Amer. Chem. Soc., 89, 3073 (1967).
21. O'Brien, R.J. and Myer, G.H., J. Chem. Phys., 53, 3832 (1970).
22. Becker, K.H., Groth, W. and Schurath, U., Chem. Phys. Lett., 8, 259 (1971).

23. Arnold, S.J., Kubo, M. and Ogryzlo, E.A., Advan. Chem. Ser., 77, 133 (1969).
24. Stuhl, F. and Welge, Can. J. Chem., 47, 2311 (1967).
25. Izod, T.P. and Wayne, R.D., Proc. Roy. Soc., A308, 81 (1968).
26. Davidson, J.A. and Ogryzlo, E.A., in "Chemiluminescence and Bioluminescence", Cormier, M.J., Hercules, D.M. and Lee, J. (Eds.), Plenum Press, N.Y. (1973).
27. Ackerman, R.A., Rosenthal, I. and Pitts, J.N., in press.
28. Furukawa, K. and Ogryzlo, E.A., J. Photochem., 1, 163 (1972).
29. Findlay, F.D., Fortin, C.J. and Snelling, D.R., Chem. Phys. Letts., 3, 204 (1969).
30. Clark, I.D. and Wayne, R.P., Chem. Phys. Letts., 3, 93 (1969).
31. Merkel, P.B. and Kearns, D.R., J. Amer. Chem. Soc., 94, 7244 (1972).
32. Ackerman, R.A., Pitts, J.M. and Steer, R.P., J. Chem. Phys., 52, 1603 (1970).
33. Ogryzlo, E.A. and Tang, C.W., J. Amer. Chem. Soc., 92, 5034 (1970).
34. Gollnick, K., Advan. Photochem., 6, 1 (1968).
35. Trozzolo, A.M. (Ed.), "Singlet Molecular Oxygen and Its Role in Environmental Sciences", Ann., N.Y., Acad. Sci., 171, 1 (1970).
36. Foote, C.S., Acct. Chem. Res., 1, 104 (1968).
37. Foote, C.S., Science, 162, 963 (1968).
38. Gollnick, K. Advan. Chem. Series, 77, 78 (1968).
39. Litt, F.A. and Nickon, A., Advan. Chem. Ser., 77, 118 (1968).
40. Nickon, A. and Mendelson, W.L., J. Amer. Chem. Soc., 87, 3921 (1965).
41. Nickon, A., DiGiorgio, J.B., and Daniels, P.J.L., J. Org. Chem., 38, 533 (1973).

42. Kearns, D.R., Fenical, W. and Radlick, P., Ann. N.Y. Acad. Sci., 171, 34 (1970).
43. Kopecky, V.R. and Reich, H.H., Can. J. Chem., 43, 2265 (1965).
44. Fenical, W., Kearns, D.R. and Radlick, P., J. Amer. Chem. Soc., 91, 7771 (1969).
45. Kearns, D.R., J. Amer. Chem. Soc., 91, 6554 (1969).
46. Kopecky, K.R. and Mumford, C., Can. J. Chem., 47, 709 (1969).
47. Foote, C.S., Fujimoto, T.T., and Chang, Y.C., Tett. Letts., 45 (1972).
48. Young, R.H., Wehrly, K. and Martin, R.L., J. Amer. Chem. Soc., 93, 5774 (1971).
49. Young, R.H., Martin, R.L., Chinh, N., Mallon, C. and Kayser, R.H., Can. J. Chem., 50, 932 (1972).
50. Furukawa, K., Gray, E.W., and Ogryzlo, E.A., Ann. N.Y. Acad. Sci., 171, 175 (1970).
51. Furukawa, K. and Ogryzlo, E.A., Chem. Phys. Letts., 12, 370 (1971).
52. Ackerman, R.A., Pitts, J.N., and Rosenthal, I. "Symposium on Oxidation by Singlet Oxygen", American Chemical Society, Washington, D.C. (1971).
53. Herron, J.H. and Huie, R.E., Environ. Sci. Tech., 4, 685 (1970).
54. Herron, J.H. and Huie, R.E., Ann. N.Y. Acad. Sci., 171, 229 (1970).
55. Hollinden, G.A. and Timmons, R.B., J. Amer. Chem. Soc., 92, 4180 (1970).
56. Ackerman, R.A., Pitts, J.N. and Steer, R.D., Chem. Phys. Letts., 12, 526 (1972).
57. Herron, J.H. and Huie, R.E., "Symposium on Oxidation by Singlet Oxygen", American Chemical Soc., Washington, D.C. (1971).

58. Gleason, W.S., Broadbent, A.D., Whittle, E. and Pitts, J.N.,  
J. Amer. Chem. Soc., 92, 2068 (1968).
59. Elias, L., Ogryzlo, E.A. and Schiff, H.I., Can. J. Chem., 37,  
1680 (1959).
60. Arnold, J.S., Browne, R.J. and Ogryzlo, E.A., Photochem. and  
Photobiol., 4, 963 (1965).
61. Kreysig, E., "Advanced Engineering Mathematics", 2nd. Ed., J. Wiley  
and Sons, Inc., N.Y. (1962).
62. Alger, R.S., "Electron Paramagnetic Resonance", J. Wiley and Sons,  
Inc., N.Y. (1968).
63. Koch, E., Tetrahedron, 24, 6295 (1968).
64. Schenk, G.O. and Koch, E., Z. Electrochem., 64, 170 (1960).
65. Wilke, C.R. and Chang, P., Amer. Inst. Chem. Eng. J., 1, 264 (1955).
66. Foote, C.S. and Denny, R.W., J. Amer. Chem. Soc., 93, 5162 (1971).
67. Foote, C.S. and Denny, R.W., J. Amer. Chem. Soc., 93, 5168 (1971).
68. Wasserman, A., "Diels-Alder Reactions", Elsevier, N.W. (1965).
69. Benson, S.W., "The Foundations of Chemical Kinetics", McGraw Hill,  
N.Y. (1960).
70. Benson, S.W., "Thermochemical Kinetics", John Wiley & Sons, N.Y. (1968).
71. American Petroleum Institute Research Project 44. Thermodynamics  
Research Center, Texas (1972).
72. Laidler, "Chemical Kinetics", 2nd. Ed., McGraw-Hill, N.Y. (1965).
73. Herron, J.H. and Huie, R.E., Int. J. Chem. Kin., 5, 193 (1973).